The ultraweak-local discontinuous Galerkin method for extended Fisher-Kolmogorov equations

Fengyu Fu[*], Chi-Wang Shu[†], Qi Tao[‡]

Abstract: The extended Fisher-Kolmogorov (EFK) equation serves as a fundamental model in biophysics, fluid dynamics, and chemical-reaction diffusion systems. This paper investigates the ultraweak-local discontinuous Galerkin (UWLDG) method for solving the initial boundary value problem of the EFK equation. The UWLDG schemes are specifically designed to accommodate four distinct types of non-periodic boundary conditions. These schemes are proved to be energy stable and of optimal order $k+1$ using piecewise polynomials of degree k ($k \geq 1$), applicable in both one- and two-dimensional settings. The alternating numerical flux and the delicate boundary numerical flux are employed to effectively match the different types of boundary conditions. A key ingredient in the derivation of the optimal error estimates is the construction of appropriate projections and the handling of nonlinear error terms without the aid of a priori assumptions. Numerical experiments are presented to verify the sharpness of our theoretical findings and to demonstrate the effectiveness of the UWLDG schemes in solving EFK problems with small parameters.

Keywords: Extended Fisher-Kolmogorov equation, Ultraweak-local discontinuous Galerkin method, Non-periodic boundary conditions, Energy stability, Optimal error estimates.

1 Introduction

In this paper, we study the ultraweak-local discontinuous Galerkin (UWLDG) method for the following time-dependent nonlinear fourth-order equation

$$u_t - \Delta u + \gamma \Delta^2 u + f(u) = 0, \quad (\boldsymbol{x}, t) \in \Omega \times (0, T], \tag{1.1}$$

with the initial condition

$$u(\boldsymbol{x}, 0) = u_0(\boldsymbol{x}), \quad \boldsymbol{x} \in \Omega, \tag{1.2}$$

[*]College of Science, Harbin University of Science and Technology, Harbin 150080, Heilongjiang, China. Email: fengyu_fu@hrbust.edu.cn. The research of the first author was supported by the Fundamental Research Foundation for Universities of Heilongjiang Province grant 217045543.

[†]Division of Applied Mathematics, Brown University, Providence, RI 02912, Email: chi-wang_shu@brown.edu. The research of the second author was supported by NSF grant DMS-2309249.

[‡]Corresponding author. School of Mathematics, Statistics and Mechanics, Beijing University of Technology, Beijing 100124, China, Email: taoqi@bjut.edu.cn. The research of the third author was supported by NSFC grant 12301464.

and non-periodic boundary conditions, which will be specified later. In (1.1), $f(u) = u^3 - u$ represents the nonlinear term, γ denotes a positive constant dictated by physical requirements, Δ represents the Laplacian operator and $\Omega \subset \mathbb{R}^d$ $(d \geq 1)$ defines a bounded Cartesian domain with boundary $\partial\Omega$.

Equation (1.1) is known as the extended Fisher-Kolmogorov (EFK) equation, as it simplifies to the standard Fisher-Kolmogorov (FK) equation [17, 23] when $\gamma = 0$. However, the FK equation can exhibit less stable behavior in certain contexts, especially in the study of bistability of traveling waves in chemical systems [31]. To enhance the stability of the FK equation and extend its applicability to a broad range of biophysical and chemical models, Coullet et al. [8], Dee and Van Saarloos [13, 31] formulated the EFK equation (1.1) by incorporating a stabilizing fourth-order derivative term $\gamma\Delta^2 u$ into the FK equation. The EFK model is more sophisticated and can accurately characterize much more complex phenomena. It has demonstrated significant utility in various fields, including traveling waves in reaction diffusion systems [1, 2], pattern formation in bistable systems [13, 26], mesoscopic models of phase transitions in binary systems near the Lifshitz point [20, 34], and the propagation of domain walls in liquid crystals [33]. In particular, during phase transitions near Lifshitz points, fourth-order derivative terms play a crucial role, especially in describing the stability of the modulated phase and constructing the phase diagram [34]. For further study on the dynamics of the EFK equations, we refer to the works in [27, 28].

However, the inclusion of higher-order spatial derivative operators and nonlinear terms in the EFK equation presents significant challenges in obtaining analytical solutions. To numerically investigate the EFK problem, we are interested in considering the following four types of boundary conditions:

- The generalized Dirichlet boundary condition (G-Dirichlet B.C.)

$$u = f_D, \qquad \Delta u = g_D, \quad \text{on } \partial\Omega; \tag{1.3a}$$

- The Dirichlet boundary condition (Dirichlet B.C.)

$$u = f_D, \qquad \frac{\partial u}{\partial \boldsymbol{\nu}} = f_N, \quad \text{on } \partial\Omega; \tag{1.3b}$$

- The Neumann boundary condition (Neumann B.C.)

$$\frac{\partial u}{\partial \boldsymbol{\nu}} = f_N, \qquad \frac{\partial \Delta u}{\partial \boldsymbol{\nu}} = g_N, \quad \text{on } \partial\Omega; \tag{1.3c}$$

- The mixed boundary condition (mixed B.C.)

$$\begin{aligned} u &= f_D, && \Delta u = g_D, && \text{on } \Gamma_D, \\ \frac{\partial u}{\partial \boldsymbol{\nu}} &= f_N, && \frac{\partial \Delta u}{\partial \boldsymbol{\nu}} = g_N, && \text{on } \Gamma_N, \end{aligned} \tag{1.3d}$$

where $\boldsymbol{\nu}$ is the unit outward normal vector to the boundary $\partial\Omega$. Γ_D and Γ_N in (1.3d) are subsets of $\partial\Omega$ that satisfy $\Gamma_D \cup \Gamma_N = \partial\Omega$ and $\Gamma_D \cap \Gamma_N = \emptyset$. We assume that $u_0(\boldsymbol{x})$, f_D, g_D, f_N, g_N are sufficiently smooth functions such that problem (1.1) admits a unique exact solution. The existence, uniqueness and regularity results of weak solutions to the equation (1.1) with the boundary conditions in (1.3) were discussed in [9, 11, 19].

The development of effective numerical methods for the EFK model under various boundary conditions has attracted significant attention in recent years. Most of the existing theoretical

results concentrate on periodic or homogeneous boundary conditions. For example, an adaptive low-rank splitting approach was proposed in [32] for the EFK equation with periodic boundary condition. Several finite difference methods have been studied for the EFK problems with the homogeneous boundary condition (1.3a), including the Crank-Nicolson type second-order scheme [21, 22] and a novel fourth-order compact finite difference scheme [24]. In the context of finite element methods (FEM), a C^1 conforming FEM was developed in [11] for the EFK equation with (1.3a) and (1.3b), achieving optimal error estimates for semi- and fully-discrete schemes. Subsequently, a fully discrete C^0 interior penalty FEM was formulated and analyzed in [19] for the EFK problem with (1.3c). Furthermore, a mixed FEM [12], an H^1-Galerkin mixed FEM [16], and a finite element Galerkin method [9] was developed for the EFK equation with (1.3a). Additionally, a nonconforming FEM employing Bergan's energy-orthogonal element [25] was also proposed and analyzed for the EFK equation with (1.3a), achieving optimal estimates of order $O(h)$ in the energy norm. However, to our knowledge, there appears to be a notable absence of literature on the application of discontinuous Galerkin (DG) methods to investigate the EFK problem, especially on the analysis concerning non-homogeneous boundary conditions specified in (1.3a)–(1.3d).

As an effective numerical method to deal with problems with high-order derivatives, the local discontinuous Galerkin (LDG) method was first proposed in [7] and has been applied in a wide range of applications [14, 29]. In 2008, another novel approach for approximating equations with high-order derivatives, known as the ultraweak discontinuous Galerkin (UWDG) method [5]. In 2020, Tao, Xu and Shu introduced a new class of DG methods that inherit the advantages of both the LDG and UWDG methodologies. This innovative approach, termed the UWLDG method [30], is specifically designed to solve partial differential equations with high-order spatial derivatives. The UWLDG scheme is constructed in two steps: first, by properly introducing auxiliary variables, the high-order equation is strategically transformed into a system of relatively lower order (though not entirely first-order); second, the UWDG approach is applied to each of these lower-order equations through a careful selection of numerical fluxes. For equations of fourth-order and higher, the UWLDG method exhibits superior efficiency compared to both the LDG and UWDG methods, as it introduces fewer auxiliary variables and does not require internal penalty terms to ensure stability.

In this paper, we investigate the optimal error estimates of the UWLDG method for one- and two-dimensional EFK equations (1.1) under boundary conditions specified in (1.3). We begin by transforming the EFK equation into two second-order equations through the introduction of a proper auxiliary variable; and then design the alternating interior numerical fluxes and subtle boundary fluxes by utilizing the information of the exact boundary conditions in a careful manner. Next, we establish the energy stability of the proposed semi-discrete UWLDG schemes. In particular, we have proven the optimal error estimates in the L^2-norm for both the primary solution and the auxiliary variables of one- and two-dimensional EFK problems. These optimal error estimates are achieved without relying on the technique of a priori assumptions, thereby establishing the estimation of nonlinear error terms within a robust and rigorous framework. Furthermore, a crucial component of our methodology is the construction of suitable projections as well as an exploration of their superconvergent property. This superconvergence plays a vital role in enhancing the overall theoretical accuracy of our numerical approach.

This paper is organized as follows. In Section 2, we present the UWLDG scheme and show the stability as well as optimal error estimates for the one-dimensional EFK problem (1.1) with boundary conditions (1.3a)–(1.3d). In Section 3, we extend these theoretical results to

the two-dimensional case on a Cartesian mesh, in which numerical boundary conditions and projections are carefully analyzed. In Section 4, we provide numerical experiments to confirm the theoretical findings. Some concluding remarks are given in Section 5. Finally, in Appendix A, we provide the proofs of a few technical lemmas.

Throughout the paper, we use the standard notation for Sobolev spaces and norms. Specifically, let $W^{m,p}(D)$ be the Sobolev space in D equipped with the norm $\|\cdot\|_{m,p,D}$, then for $p=2$, we simplify $W^{m,2}(D)$ to $H^m(D)$, and the norm $\|\cdot\|_{m,2,D}$ to $\|\cdot\|_{m,D}$. For any partition Ω_h of the domain Ω and any integer $l \geq 0$, the broken Sobolev space $H^\ell(\Omega_h)$ refers to a space where the functions are in the space $L^2(\Omega)$ and are Sobolev H^ℓ on each element of Ω_h, with associated norms defined piecewisely. We denote $\|\cdot\|_{\ell,2,\Omega_h}$ by $\|\cdot\|_\ell$ for clarity when there is no confusion. The L^2 norm in D is represented by $\|\cdot\|_D$, and we omit the subscript D when $D=\Omega$ or Ω_h.

2 The one-dimensional UWLDG scheme

To clarify the UWLDG scheme, we will start with the one-dimensional case in this section. We consider the following one-dimensional EFK equation:

$$u_t - u_{xx} + \gamma u_{xxxx} + f(u) = 0, \quad (x,t) \in [a,b] \times (0,T], \tag{2.1}$$

with the initial condition

$$u(x,0) = u_0(x), \quad x \in (a,b), \tag{2.2}$$

and the boundary conditions (1.3a)–(1.3d). In one-dimensional case we denote

$$\frac{\partial^i u}{\partial x^i}(a,t) = f_i(t), \quad \frac{\partial^i u}{\partial x^i}(b,t) = g_i(t), \quad i = 0,1,2,3. \tag{2.3}$$

We assume that $u_0(x)$, $f_i(t)$, $g_i(t)$, $i=0,1,2,3$ are sufficiently smooth functions.

Before presenting the UWLDG scheme, we first introduce some notation that will be used in its formulation. First, we divide the computational domain $\Omega=[a,b]$ into N cells

$$a = x_{\frac{1}{2}} < x_{\frac{3}{2}} < \cdots < x_{N+\frac{1}{2}} = b,$$

and denote

$$I_j = \left(x_{j-\frac{1}{2}},\ x_{j+\frac{1}{2}}\right), \quad h_j = x_{j+\frac{1}{2}} - x_{j-\frac{1}{2}}, \quad \Omega_h = \{I_j\},$$

as the cells, cell lengths and the partition of Ω, respectively. We also define $h = \max_j h_j$ and assume that the mesh is regular. We take the following piecewise polynomial finite element space

$$V_h = \{v \in L^2(\Omega) : v|_{I_j} \in \mathcal{P}^k(I_j),\ j \in Z_N\}, \quad Z_N = \{1,\ldots,N\},$$

where $\mathcal{P}^k(I_j)$ denotes the space of polynomials in I_j of degree at most k . We use $(v_h)^-_{j+\frac{1}{2}}$ and $(v_h)^+_{j+\frac{1}{2}}$ to denote the value of v_h at $x_{j+\frac{1}{2}}$ from the left and right cells, respectively. Furthermore, the jump of v_h at $x_{j+\frac{1}{2}}$ is defined as

$$[\![v_h]\!]_{j+\frac{1}{2}} = (v_h)^+_{j+\frac{1}{2}} - (v_h)^-_{j+\frac{1}{2}}.$$

2.1 The UWLDG scheme

To construct the UWLDG scheme, we first introduce an auxiliary variable w and two parameters α and β to rewrite the EFK equation (2.1) into a second-order system:

$$\begin{aligned} &u_t - \alpha w + \beta w_{xx} + \widetilde{f}(u) = 0, \\ &w + \alpha u - \beta u_{xx} = 0, \end{aligned}$$

where $\alpha = \frac{1}{2\sqrt{\gamma}},\ \beta = \sqrt{\gamma}$, and the nonlinear term in the rewritten formulation is changed to $\widetilde{f}(u) = u^3 - \big(1 + \frac{1}{4\gamma}\big)u$. Then, the UWLDG scheme is defined as follows: find $u_h, w_h \in V_h$, such that for any $p, q \in V_h$ and $j \in Z_N$, we have

$$\big((u_h)_t, p\big)_j - \alpha(w_h, p)_j + \beta \mathcal{D}_j(w_h, p) + \big(\widetilde{f}(u_h), p\big)_j = 0, \tag{2.4a}$$

$$(w_h, q)_j + \alpha(u_h, q)_j - \beta \mathcal{D}_j(u_h, q) = 0, \tag{2.4b}$$

where $(u, v)_j = \int_{I_j} uv\ dx$ and

$$\mathcal{D}_j(v, p) = (v, p_{xx})_j + \widehat{v_x} p^-|_{j+\frac{1}{2}} - \widehat{v_x} p^+|_{j-\frac{1}{2}} - \widehat{v} p_x^-|_{j+\frac{1}{2}} + \widehat{v} p_x^+|_{j-\frac{1}{2}}, \quad \forall v \in H^2(\Omega_h),\ p \in V_h.$$

The hat terms $\widehat{u_h},\ \widehat{(u_h)_x},\ \widehat{w_h},\ \widehat{(w_h)_x}$ in the scheme (2.4a)-(2.4b) are numerical fluxes.

The main idea of designing numerical fluxes is similar to [18]. At the interior points, we choose the alternating fluxes for all four kinds of boundary conditions in (1.3a)–(1.3d):

$$\big(\widehat{u_h},\ \widehat{(u_h)_x},\ \widehat{w_h},\ \widehat{(w_h)_x}\big)_{j+\frac{1}{2}} = \big(u_h^+,\ (u_h)_x^-,\ w_h^+,\ (w_h)_x^-\big)_{j+\frac{1}{2}}, \quad j = 1, \ldots, N-1, \tag{2.5}$$

where $\widehat{u_h}$ and $\widehat{(w_h)_x}$ take the opposite sides, and $\widehat{(u_h)_x}$ and $\widehat{w_h}$ take the opposite sides. At the boundary points $x_{\frac{1}{2}},\ x_{N+\frac{1}{2}}$, the numerical fluxes are defined according to different boundary conditions:

• For the G-Dirichlet B.C.:

$$\big(\widehat{u_h},\ \widehat{(u_h)_x},\ \widehat{w_h},\ \widehat{(w_h)_x}\big)_{\frac{1}{2}} = \big(f_0(t),\ \ (u_h)_x^+,\ \ -\alpha f_0(t) + \beta f_2(t),\ \ (w_h)_x^+\big)_{\frac{1}{2}}, \tag{2.6a}$$

$$\big(\widehat{u_h},\ \widehat{(u_h)_x},\ \widehat{w_h},\ \widehat{(w_h)_x}\big)_{N+\frac{1}{2}} = \big(g_0(t),\ \ (u_h)_x^-,\ \ -\alpha g_0(t) + \beta g_2(t),\ \ (w_h)_x^-\big)_{N+\frac{1}{2}}. \tag{2.6b}$$

• For the Dirichlet B.C.:

$$\big(\widehat{u_h},\ \widehat{(u_h)_x},\ \widehat{w_h},\ \widehat{(w_h)_x}\big)_{\frac{1}{2}} = \big(f_0(t),\ \ f_1(t),\ \ w_h^+,\ \ (w_h)_x^+ - \frac{k_2}{h^3}[\![u_h]\!]\big)_{\frac{1}{2}}, \tag{2.7a}$$

$$\big(\widehat{u_h},\ \widehat{(u_h)_x},\ \widehat{w_h},\ \widehat{(w_h)_x}\big)_{N+\frac{1}{2}} = \big(g_0(t),\ \ g_1(t),\ \ w_h^- + \frac{k_1}{h}[\![(u_h)_x]\!],\ \ (w_h)_x^-\big)_{N+\frac{1}{2}}, \tag{2.7b}$$

where $k_1,\ k_2$ are positive constants, and we set

$$(u_h)_{\frac{1}{2}}^- := f_0(t), \quad (u_h)_{N+\frac{1}{2}}^+ := g_0(t), \quad \big((u_h)_x\big)_{\frac{1}{2}}^- := f_1(t), \quad \big((u_h)_x\big)_{N+\frac{1}{2}}^+ := g_1(t),$$

to ensure that the penalty terms are well-defined.

• For the Neumann B.C.:

$$\big(\widehat{u_h},\ \widehat{(u_h)_x},\ \widehat{w_h},\ \widehat{(w_h)_x}\big)_{\frac{1}{2}} = \big(u_h^+,\ \ f_1(t),\ \ w_h^+,\ \ -\alpha f_1(t) + \beta f_3(t)\big)_{\frac{1}{2}}, \tag{2.8a}$$

$$\big(\widehat{u_h},\ \widehat{(u_h)_x},\ \widehat{w_h},\ \widehat{(w_h)_x}\big)_{N+\frac{1}{2}} = \big(u_h^-,\ \ g_1(t),\ \ w_h^-,\ \ -\alpha g_1(t) + \beta g_3(t)\big)_{N+\frac{1}{2}}. \tag{2.8b}$$

• For the mixed B.C.:

$$\big(\widehat{u_h},\ \widehat{(u_h)_x},\ \widehat{w_h},\ \widehat{(w_h)_x}\big)_{\frac{1}{2}} \quad = \big(u_h^+,\ \ f_1(t),\ \ w_h^+,\ \ -\alpha f_1(t)+\beta f_3(t)\big)_{\frac{1}{2}}, \tag{2.9a}$$

$$\big(\widehat{u_h},\ \widehat{(u_h)_x},\ \widehat{w_h},\ \widehat{(w_h)_x}\big)_{N+\frac{1}{2}} = \big(g_0(t),\ \ (u_h)_x^-,\ \ -\alpha g_0(t)+\beta g_2(t),\ \ (w_h)_x^-\big)_{N+\frac{1}{2}}. \tag{2.9b}$$

Furthermore, we omit the subscript j in equations (2.4a)-(2.4b) to denote the summation over all j. After summing the variational formulations (2.4a)-(2.4b) over all cells, we obtain the UWLDG scheme in the global form:

$$\big((u_h)_t,p\big)-\alpha(w_h,p)+\beta\mathcal{D}(w_h,p)+\big(\widetilde{f}(u_h),p\big)=0, \tag{2.10a}$$

$$(w_h,q)+\alpha(u_h,q)-\beta\mathcal{D}(u_h,q)=0. \tag{2.10b}$$

Remark 2.1. *The choice of numerical flux is not unique for each type of boundary condition, and we refer to [18, Remark 2.1 and 2.2] for more details. It should be noted that the design of* $\widehat{w_h}$ *and* $\widehat{(w_h)_x}$ *at the boundary points with actual boundary conditions differs from that in [18], due to the different definition of the auxiliary variable* w.

2.2 Energy stability of the UWLDG scheme

In this subsection, we will demonstrate the energy stability of the scheme (2.4) with the numerical fluxes (2.5)–(2.9).

Theorem 2.2. *We assume the EFK problem* (2.1) *equipped with the homogeneous boundary conditions* (1.3)*, then*

- *the UWLDG solutions* u_h*,* w_h *obtained by scheme* (2.4) *with the interior numerical flux* (2.5) *and the boundary flux* (2.6)*, or* (2.8), (2.9)*, satisfy the following stability*

$$\frac{d}{dt}\int_{\Omega_h}\Big(\frac{1}{2}w_h^2+\widetilde{F}(u_h)\Big)dx\le 0; \tag{2.11}$$

- *the UWLDG solutions* u_h*,* w_h *obtained by scheme* (2.4) *with the interior numerical flux* (2.5) *and boundary flux* (2.7)*, satisfy the following stability*

$$\frac{d}{dt}\Big(\int_{\Omega_h}\frac{1}{2}w_h^2+\widetilde{F}(u_h)\,dx+\frac{\beta}{2}S(u_h)\Big)\le 0, \tag{2.12}$$

where

$$\widetilde{F}(u_h)=\frac{1}{4}\Big(u_h^2-\big(1+\frac{1}{4\gamma}\big)\Big)^2,\quad S(u_h)=\frac{k_1}{h}\Big((u_h)_x\big(x^-_{N+\frac{1}{2}}\big)\Big)^2+\frac{k_2}{h^3}\Big(u_h(x^+_{\frac{1}{2}})\Big)^2. \tag{2.13}$$

Proof. Firstly, we take the time derivative of (2.10b) and choose the test function $q=w_h$. Then, we choose $p=(u_h)_t$ in (2.10a), and add the two equations together to obtain

$$\big((u_h)_t,(u_h)_t\big)+\big((w_h)_t,w_h\big)+\big(\widetilde{f}(u_h),(u_h)_t\big)+\beta\mathcal{D}(w_h,(u_h)_t)-\beta\mathcal{D}\big((u_h)_t,w_h\big)=0, \tag{2.14}$$

where $\widehat{(u_h)_t}:=(\widehat{u_h})_t$ in $\mathcal{D}\big((u_h)_t,w_h\big)$. Notice that

$$\big(\widetilde{f}(u_h),(u_h)_t\big)=\frac{d}{dt}\int_{\Omega_h}\widetilde{F}(u_h)dx, \tag{2.15}$$

where $\widetilde{F}(u_h)$ is defined in (2.13). Then we get

$$\frac{d}{dt}\int_{\Omega_h}\Big(\frac{1}{2}w_h^2+\widetilde{F}(u_h)\Big)dx+\beta\mathcal{D}\big(w_h,(u_h)_t\big)-\beta\mathcal{D}\big((u_h)_t,w_h\big)=-\int_{\Omega_h}(u_h)_t^2dx\le 0. \tag{2.16}$$

Thanks to the definition of the alternating numerical flux (2.5) and homogeneous boundary conditions, we have

$$\mathcal{D}(w_h,(u_h)_t)-\mathcal{D}\big((u_h)_t,w_h\big)=0 \tag{2.17}$$

for the boundary fluxes (2.6), (2.8), and (2.9); and

$$\mathcal{D}\big(w_h,(u_h)_t\big)-\mathcal{D}\big((u_h)_t,w_h\big)=\frac{1}{2}\frac{d}{dt}S(u_h) \tag{2.18}$$

for the boundary flux (2.7). Therefore, we obtain (2.11) and (2.12).

□

2.3 A priori error estimates

In this subsection, we consider the error estimate of the UWLDG scheme (2.4) for solving the EFK equation (2.1) with different types of boundary conditions specified in (1.3).

2.3.1 Projections

First of all, we give the definitions of several basic projections that will be used to construct the projections tailored to different boundary conditions in the error estimates. Given $u\in H^2(\Omega_h)$, we define three kind of one-dimensional projections into V_h as follows.

- P_1: For $k\ge 1$, $j\in Z_N$, $\mathsf{P}_1u|_{I_j}\in\mathcal{P}^k(I_j)$, such that

$$\int_{I_j}(u-\mathsf{P}_1u)v_h\,dx=0,\quad \forall v_h\in\mathcal{P}^{k-2}(I_j), \tag{2.19a}$$

$$\mathsf{P}_1u\big(x^+_{j-\frac{1}{2}}\big)=u\big(x_{j-\frac{1}{2}}\big),\quad \big(\mathsf{P}_1u\big)_x\big(x^-_{j+\frac{1}{2}}\big)=u_x\big(x_{j+\frac{1}{2}}\big). \tag{2.19b}$$

- P_2: For $k\ge 1$, $j\in Z_N$, $\mathsf{P}_2u|_{I_j}\in\mathcal{P}^k(I_j)$, such that

$$\int_{I_j}(u-\mathsf{P}_2u)v_h\,dx=0,\quad \forall v_h\in\mathcal{P}^{k-2}(I_j), \tag{2.20a}$$

$$\mathsf{P}_2u\big(x^+_{j-\frac{1}{2}}\big)=u\big(x_{j-\frac{1}{2}}\big),\quad \mathsf{P}_2u\big(x^-_{j+\frac{1}{2}}\big)=u\big(x_{j+\frac{1}{2}}\big). \tag{2.20b}$$

- P_3: For $k\ge 2$, $j\in Z_N$, $\mathsf{P}_3u|_{I_j}\in\mathcal{P}^k(I_j)$, such that

$$\int_{I_j}(u-\mathsf{P}_3u)v_h\,dx=0,\quad \forall v_h\in\mathcal{P}^{k-2}(I_j), \tag{2.21a}$$

$$(\mathsf{P}_3u)_x\big(x^+_{j-\frac{1}{2}}\big)=u_x\big(x_{j-\frac{1}{2}}\big),\quad (\mathsf{P}_3u)_x\big(x^-_{j+\frac{1}{2}}\big)=u_x\big(x_{j+\frac{1}{2}}\big). \tag{2.21b}$$

Then, to analyze the error estimates of the UWLDG schemes for different boundary conditions, we construct the projections $\mathbb{P}_{\mathrm{I}}$, $\mathbb{P}_{\mathrm{II}}$, $\mathbb{P}_{\mathrm{III}}$ based on the definitions of projections P_1, P_2, and P_3,

as follows:

$$\mathbb{P}_{\rm I} : \mathbb{P}_{\rm I}|_{I_1} = \mathsf{P}_3|_{I_1},\ \mathbb{P}_{\rm I}|_{I_j} = \mathsf{P}_1|_{I_j},\ j = 2, \ldots, N, \tag{2.22a}$$

$$\mathbb{P}_{\rm II} : \mathbb{P}_{\rm II}|_{I_j} = \mathsf{P}_1|_{I_j}, \quad \forall j \in Z_N, \tag{2.22b}$$

$$\mathbb{P}_{\rm III} : \mathbb{P}_{\rm III}|_{I_N} = \mathsf{P}_2|_{I_N},\ \mathbb{P}_{\rm III}|_{I_j} = \mathsf{P}_1|_{I_j},\ j = 1, 2, \ldots, N-1. \tag{2.22c}$$

It is easy to verify that all these projections are well defined and possess the following optimal approximation property; see [6, 30].

Lemma 2.3. *Let π be any projection defined by* (2.22a)–(2.22c)*, then for $u \in H^{k+1}(\Omega_h)$, there holds*

$$\|u - \pi u\| + h^{\ell}\|u - \pi u\|_{\ell} + h^{\frac{1}{2}}\|u - \pi u\|_{\Gamma_h} \le Ch^{k+1}\|u\|_{k+1}, \tag{2.23}$$

where $\|v\|_{\Gamma_h} = \Big(\sum_{j=1}^{N}\big[(v^-_{j+\frac{1}{2}})^2 + (v^+_{j-\frac{1}{2}})^2\big]\Big)^{\frac{1}{2}}$, $1 \le \ell \le k$ is an integer and C is a positive constant independent of h.

2.3.2 Error estimates

In this subsection, we take the G-Dirichlet B.C. as an example to demonstrate the error estimates of the UWLDG scheme for the EFK problem. The boundary condition analysis of the UWLDG method for linear fourth-order problems has been presented in [18], in which optimal error estimates were derived. In the current paper, we follow the proof strategy for error estimates from [18], while paying particular attention to addressing the nonlinear error terms generated by the nonlinear function $f(u)$. By integrating these techniques, the results can be readily extended to the other three boundary conditions.

To facilitate the estimation of nonlinear terms in the error analysis, we first establish the following lemma.

Lemma 2.4. *Suppose $k \ge 1$, the function $s(t) \ge 0$ satisfies $s(0) \le Ch^{2k+2}$ and the following inequality*

$$s'(t) \le C(h^{-2}s^2 + s + h^{2k+2}), \quad 0 \le t \le T, \tag{2.24}$$

where C is a constant independent of h and t. Then, when h is small enough, we have

$$s(t) \le \widetilde{C}h^{2k+2}, \quad 0 \le t \le T,$$

where $\widetilde{C}$ is a constant independent of h and dependent on T.

Proof. The proof of this lemma is given in Appendix A.1. □

Theorem 2.5. *Let u be the exact solution of the EFK equation* (2.1) *subject to the G-Dirichlet B.C.* (1.3a)*, $w = -\alpha u + \beta u_{xx}$. We assume u is sufficiently smooth, e.g., $\|u\|_{k+5}, \|u_t\|_{k+1}$ are bounded uniformly for any time t. Let u_h, w_h be solutions of the UWLDG scheme* (2.4) *with numerical fluxes* (2.5)–(2.6)*. Then, for $k > 1$, we have the following optimal error estimates:*

$$\|u(t) - u_h(t)\| + \int_0^t \|w(\tau) - w_h(\tau)\|\, d\tau \le Ch^{k+1}, \tag{2.25}$$

where C is a constant independent of h and dependent on $\|u\|_{k+5}$, $\|u_t\|_{k+1}$, and t.

Proof. Let $e_u = u - u_h,\ e_w = w - w_h$. Since the exact solutions u and w also satisfy the UWLDG scheme (2.4)-(2.6), we have

$$\big((e_u)_t, p\big) - \alpha(e_w, p) + \beta\mathcal{D}(e_w, p) + \big(\widetilde{f}(u) - \widetilde{f}(u_h), p\big) = 0, \tag{2.26a}$$

$$(e_w, q) + \alpha(e_u, q) - \beta\mathcal{D}(e_u, q) = 0. \tag{2.26b}$$

According to the G-Dirichlet B.C. (1.3a) and the boundary numerical flux (2.6), we have

$$\widehat{e_u}|_{j+\frac{1}{2}} = 0, \quad \widehat{e_w}|_{j+\frac{1}{2}} = 0, \quad j = 0,\, N. \tag{2.27}$$

Next, we choose the projection $\mathbb{P}_{\mathrm{I}}$ defined by (2.22a) and denote

$$\begin{aligned} e_u &= (u - \mathbb{P}_{\mathrm{I}}u) - (u_h - \mathbb{P}_{\mathrm{I}}u) := \eta_u - \xi_u, \\ e_w &= (w - \mathbb{P}_{\mathrm{I}}w) - (w_h - \mathbb{P}_{\mathrm{I}}w) := \eta_w - \xi_w. \end{aligned}$$

From (2.27), we have

$$\widehat{\xi_u}|_{j+\frac{1}{2}} = 0, \ \ \widehat{\xi_w}|_{j+\frac{1}{2}} = 0, \ \ \widehat{\eta_u}|_{j+\frac{1}{2}} = 0, \ \ \widehat{\eta_w}|_{j+\frac{1}{2}} = 0, \quad j = 0,\, N. \tag{2.28}$$

Then, taking $p = \xi_u$, $q = \xi_w$ and adding the two equations in (2.26), we get

$$\begin{aligned} &\big((\xi_u)_t, \xi_u\big) + (\xi_w, \xi_w) + \beta\big(\mathcal{D}(\xi_w, \xi_u) - \mathcal{D}(\xi_u, \xi_w)\big) \\ =&\big((\eta_u)_t, \xi_u\big) + (\eta_w, \xi_w) + \beta\big(\mathcal{D}(\eta_w, \xi_u) - \mathcal{D}(\eta_u, \xi_w)\big) + \Lambda, \end{aligned}$$

where

$$\Lambda = \big(\widetilde{f}(u) - \widetilde{f}(u_h), \xi_u\big),$$

is the nonlinear error term and will be estimated later. By (2.28) and a similar analysis to (2.17), we obtain

$$\mathcal{D}(\xi_w, \xi_u) - \mathcal{D}(\xi_u, \xi_w) = 0.$$

Besides, combining (2.28) and the definition of the projection $\mathbb{P}_{\mathrm{I}}$, we arrive at

$$\mathcal{D}(\eta_w, \xi_u) - \mathcal{D}(\eta_u, \xi_w) = 0.$$

Thus, using the optimal approximation properties given in (2.23) yields

$$\frac{1}{2}\frac{d}{dt}\|\xi_u\|^2 + \|\xi_w\|^2 = \big((\eta_u)_t, \xi_u\big) + (\eta_w, \xi_w) + \Lambda \le Ch^{k+1}(\|\xi_u\| + \|\xi_w\|) + |\Lambda|. \tag{2.29}$$

It remains to consider the estimate of Λ. Clearly,

$$\begin{aligned} \widetilde{f}(u) - \widetilde{f}(u_h) &= u^3 - \big(1 + \frac{1}{4\gamma}\big)u - u_h^3 + \big(1 + \frac{1}{4\gamma}\big)u_h \\ &= u^3 - u_h^3 - \big(1 + \frac{1}{4\gamma}\big)(u - u_h) \\ &= e_u(3u - 3ue_u + e_u^2) - \big(1 + \frac{1}{4\gamma}\big)e_u. \end{aligned}$$

A simple application of the inverse inequality and approximation properties of the projection gives us

$$\begin{aligned}|\Lambda| &= \Big|\big(e_u(3u-3ue_u+e_u^2)-\big(1+\frac{1}{4\gamma}\big)e_u,\xi_u\big)\Big| \\ &\le C\|e_u\|\|\xi_u\|(1+\|e_u\|_\infty+\|e_u\|_\infty^2) \\ &\le C(\|\xi_u\|+h^{k+1})\|\xi_u\|(1+h^{-\frac{1}{2}}\|\xi_u\|+h^{k+\frac{1}{2}}+h^{-1}\|\xi_u\|^2+h^{2k+1}) \\ &\le C\|\xi_u\|^2+Ch^{-1}\|\xi_u\|^4+Ch^{2k+2}. \end{aligned} \tag{2.30}$$

Thus, recalling (2.29), we obtain

$$\frac{1}{2}\frac{d}{dt}\|\xi_u\|^2+\frac{1}{2}\|\xi_w\|^2\le C\|\xi_u\|^2+Ch^{-1}\|\xi_u\|^4+Ch^{2k+2}. \tag{2.31}$$

Combining (2.31) with Lemma 2.4, we get

$$\|\xi_u\|\le Ch^{k+1}. \tag{2.32}$$

Then, by (2.32) and (2.31), we further have

$$\int_0^t\|\xi_w\|d\tau\le Ch^{k+1}. \tag{2.33}$$

Finally, by applying the triangle inequality, we arrive at (2.25). □

Remark 2.6. *For $k=1$, we cannot prove that the optimal error estimate result* (2.25) *holds, as the projection $\mathbb{P}_{\mathrm{I}}$ does not exist. In fact, our numerical experiments indicate that the error is only of order $\frac{3}{2}$ for both the L^2 errors $\|e_u\|$ and $\|e_w\|$. For a detailed view of these results, we refer to Tables 4.1 and 4.2 in Section 4.*

Remark 2.7. *For the EFK problem* (2.1) *subject to the Dirichlet B.C.* (1.3a)*, the Neumann B.C.* (1.3c) *or the mixed B.C.* (1.3d)*, the UWLDG solutions of the scheme* (2.4) *with the interior numerical flux* (2.5) *and the associated boundary fluxes* (2.7)–(2.9) *also satisfy the optimal error estimate* (2.25) *for $k\ge 1$. This can be proved by employing similar arguments as in the proof of Theorem 2.5, utilizing the projection $\mathbb{P}_{\mathrm{II}}$ defined by* (2.22b) *for the cases of the Dirichlet B.C. and the mixed B.C., and $\mathbb{P}_{\mathrm{III}}$ defined by* (2.22c) *for the Neumann B.C. case.*

3 Extension to two-dimensional EFK problems

In this section, we extend our UWLDG scheme to the two-dimensional EFK equation (1.1) with boundary conditions specified in (1.3a)–(1.3d). We assume that Ω is a bounded rectangular domain in $\mathbb{R}^2$, i.e., $\Omega=[a_1,b_1]\times[a_2,b_2]$, and denote

$$\Gamma_N=\{(x,y)\in\partial\Omega|x=a_1 \text{ or } y=a_2\},\quad \Gamma_D=\{(x,y)\in\partial\Omega|x=b_1 \text{ or } y=b_2\}.$$

Let $\boldsymbol{\nu}_l=(-1,0)$, $\boldsymbol{\nu}_b=(0,-1)$, $\boldsymbol{\nu}_r=(1,0)$, $\boldsymbol{\nu}_t=(0,1)$ are the unit outward normal vectors of the left, bottom, right and top boundary side of Ω respectively.

To define the UWLDG method clearly, let us first introduce some notations in the following subsection.

3.1 Notation

Let Ω_h denote the partition of the domain Ω into shape-regular rectangular elements, specifically $\Omega_h = \{K_{ij} = I_i \times J_j \mid i = 1, \ldots, N_x, j = 1, \ldots, N_y\}$. We distinguish Ω_h^I as the set of interior elements and Ω_h^0 as the set of boundary elements. The collection of all faces within this partition is denoted as $\mathscr{E}_h$. We further categorize these faces into two groups: $\mathscr{E}_h^I$, the interior faces (shared by two elements within Ω_h), and $\mathscr{E}_h^0$, the boundary faces (lying on $\partial\Omega$). The boundary and the diameter of each element K are denoted as ∂K and h_K, respectively, and we set $h = \max_K h_K$. For every $K \in \Omega_h^I$, ∂K^l, ∂K^b, ∂K^r, and ∂K^t denote the left, bottom, right, and top face of K. $\mathscr{E}_h^{0,l}$, $\mathscr{E}_h^{0,b}$, $\mathscr{E}_h^{0,r}$, and $\mathscr{E}_h^{0,t}$ denote the subsets of $\mathscr{E}_h^0$ composed by the faces located on the left, bottom, right, and top sides of the domain Ω. The finite element space associated with the mesh Ω_h is of the form

$$W_h = \left\{ v \in L^2(\Omega) : v|_K \in \mathcal{Q}^k(K),\ \forall K \in \Omega_h \right\},$$

where $\mathcal{Q}^k(K)$ is the space of tensor product of polynomials of degree at most k in each variable of $\boldsymbol{x} = (x, y)$ in K.

Besides, for a possibly discontinuous function $v(x, y)$, we define $v^{\pm}$ on the vertical and horizontal edge of an element K respectively as

$$\begin{aligned} v^{\pm}_{i+\frac{1}{2},y} &= v\big(x^{\pm}_{i+\frac{1}{2}}, y\big) = \lim_{\varepsilon \to 0^{\pm}} v\big(x_{i+\frac{1}{2}} + \varepsilon,\ y\big), \quad i = 0, 1, \ldots, N_x, \\ v^{\pm}_{x,j+\frac{1}{2}} &= v\big(x, y^{\pm}_{j+\frac{1}{2}}\big) = \lim_{\varepsilon \to 0^{\pm}} v\big(x,\ y_{j+\frac{1}{2}} + \varepsilon\big), \quad j = 0, 1, \ldots, N_y. \end{aligned}$$

And then, we denote

$$\big(\nabla v\big)^{\pm}_{i+\frac{1}{2},y} = \big((v_x)^{\pm}_{i+\frac{1}{2},y},\ \ (v_y)^{\pm}_{i+\frac{1}{2},y}\big)^{\mathsf{T}}, \quad \big(\nabla v\big)^{\pm}_{x,j+\frac{1}{2}} = \big((v_x)^{\pm}_{x,j+\frac{1}{2}},\ \ (v_y)^{\pm}_{x,j+\frac{1}{2}}\big)^{\mathsf{T}},$$

and set the jump value as

$$[\![v]\!]_{i+\frac{1}{2},y} = v^{+}_{i+\frac{1}{2},y} - v^{-}_{i+\frac{1}{2},y}, \quad [\![v]\!]_{x,j+\frac{1}{2}} = v^{+}_{x,j+\frac{1}{2}} - v^{-}_{x,j+\frac{1}{2}}.$$

3.2 The UWLDG scheme

Similar to the one-dimensional case, we rewrite (1.1) into a second order system

$$\begin{aligned} u_t - \alpha w + \beta \Delta w + \widetilde{f}(u) &= 0, \\ w + \alpha u - \beta \Delta u &= 0, \end{aligned}$$

where α, β and $\widetilde{f}(u)$ are as same as in the one-dimensional case.

The UWLDG method is given as follows: to find $u_h, w_h \in W_h$, such that

$$\big((u_h)_t, p \big)_K - \alpha (w_h, p)_K + \beta \mathcal{B}_K(w_h, p) + \big(\widetilde{f}(u_h), p\big)_K = 0, \tag{3.2a}$$

$$(w_h, q)_K + \alpha (u_h, q)_K - \beta \mathcal{B}_K(u_h, q) = 0, \tag{3.2b}$$

holds for all $p, q \in W_h$ and $K \in \Omega_h$. Here, $\mathcal{B}_K(\cdot, \cdot)$ is defined by

$$\mathcal{B}_K(v, p) := (v, \Delta p)_K + \langle \widehat{\nabla v} \cdot \mathbf{n}, p \rangle_{\partial K} - \langle \widehat{v}, \nabla p \cdot \mathbf{n} \rangle_{\partial K}, \quad \forall v \in H^2(\Omega_h),\ K \in \Omega_h, \tag{3.3}$$

where $\mathbf{n}$ denotes the unit outward normal vector to ∂K, and for any $v, z \in H^2(\Omega_h)$

$$(v,z)_K = \int_K v(x,y)z(x,y)\ dxdy, \quad \langle v, \nabla z \cdot \mathbf{n}\rangle_{\partial K} = \int_{\partial K} v(s)\big(\nabla z(s)\cdot \mathbf{n}\big)\ ds.$$

For the boundary integral in the above equation, if v or z is not single-valued on the element faces, we take its value from interior of K and restrict it on ∂K.

To complete the definition of the UWLDG method, we specify the numerical flux $\widehat{u_h}$, $\widehat{\nabla u_h}$, $\widehat{w_h}$, and $\widehat{\nabla w_h}$ for four types of boundary conditions in Table 3.1. For the interior faces $e \in \mathscr{E}_h^I$, we still choose the alternating numerical fluxes. For more details of the fluxes on the boundary faces, we refer to [18]. In Table 3.1, k_1, k_2, k_3, k_4 are positive constants and

$$\begin{aligned} u_h^-\big|_e &:= \mathbb{P}_{\mathrm{II}}(f_D)|_e, \ \forall e \in \mathscr{E}_h^{0,l}, \ \ \mathscr{E}_h^{0,b}, \\ \big((u_h)_x\big)^+\big|_e &:= \mathbb{P}_{\mathrm{II}}\big(f_N\big)|_e, \ \forall e \in \mathscr{E}_h^{0,r}, \\ \big((u_h)_y\big)^+\big|_e &:= \mathbb{P}_{\mathrm{II}}\big(f_N\big)|_e, \ \forall e \in \mathscr{E}_h^{0,t}, \end{aligned}$$

which are used to construct the four penalty terms.

Table 3.1: The numerical fluxes at the interior face $e \in \partial K^m$ and boundary face $e \in \mathscr{E}_h^{0,m}$.

Fluxes / Faces	m	$\widehat{u_h}$	$\widehat{\nabla u_h}\cdot\mathbf{n}$	$\widehat{w_h}$	$\widehat{\nabla w_h}\cdot\mathbf{n}$
Interior faces	t,r,b,l	$+$	$-$	$+$	$-$
G-Dirichlet B.C.	$t,\ r$	$\mathbb{P}_{\mathrm{I}}(f_D)$	$-$	$\mathbb{P}_{\mathrm{I}}(-\alpha f_D + \beta g_D)$	$-$
	b,l		$+$		$+$
Neumann B.C.	$t,\ r$	$-$	$\mathbb{P}_{\mathrm{III}}(f_N)$	$-$	$\mathbb{P}_{\mathrm{III}}(-\alpha f_N + \beta g_N)$
	b,l	$+$		$+$	
Mixed B.C.	$t,\ r$	$\mathbb{P}_{\mathrm{II}}(f_D)$	$-$	$\mathbb{P}_{\mathrm{II}}(-\alpha f_D + \beta g_D)$	$-$
	b,l	$+$	$\mathbb{P}_{\mathrm{II}}(f_N)$	$+$	$\mathbb{P}_{\mathrm{II}}(-\alpha f_N + \beta g_N)$
Dirichlet B.C.	t	$\mathbb{P}_{\mathrm{II}}(f_D)$	$\mathbb{P}_{\mathrm{II}}(f_N)$	$w_h^- + \frac{k_1}{h}[\![(u_h)_x]\!]$	$-$
	r			$w_h^- + \frac{k_2}{h}[\![(u_h)_y]\!]$	
	b			$+$	$(\nabla w_h)^+\cdot\boldsymbol{\nu}_m + \frac{k_3}{h}[\![u_h]\!]$
	l				$(\nabla w_h)^+\cdot\boldsymbol{\nu}_m + \frac{k_4}{h}[\![u_h]\!]$

Next, for easy presentation, we introduce

$$\begin{aligned} \mathcal{H}_{\partial K}(p,q) = &\langle w_h, \nabla(u_h)_t\cdot\mathbf{n}\rangle_{\partial K} - \langle (u_h)_t, \nabla w_h\cdot\mathbf{n}\rangle_{\partial K} + \langle \widehat{\nabla w_h}\cdot\mathbf{n}, p\rangle_{\partial K} \\ &- \langle \widehat{w_h}, \nabla p\cdot\mathbf{n}\rangle_{\partial K} - \langle (\widehat{\nabla u_h}\cdot\mathbf{n})_t, q\rangle_{\partial K} + \langle (\widehat{u_h})_t, \nabla q\cdot\mathbf{n}\rangle_{\partial K}, \end{aligned} \tag{3.4}$$

for each $K \in \Omega_h$, $p, q \in W_h$; and for $\varphi \in W_h$,

$$\begin{aligned} \mathcal{S}(\varphi) = &\sum_{j=1}^{N_y}\int_{J_j} \frac{k_1}{h}\left(\varphi_x\big(x^-_{N_x+\frac{1}{2}}, y\big)\right)^2 + \frac{k_3}{h^3}\left(\varphi\big(x^+_{\frac{1}{2}}, y\big)\right)^2 dy \\ &+ \sum_{i=1}^{N_x}\int_{I_i} \frac{k_2}{h}\left(\varphi_y\big(x, y^-_{N_y+\frac{1}{2}}\big)\right)^2 + \frac{k_4}{h^3}\left(\varphi\big(x, y^+_{\frac{1}{2}}\big)\right)^2 dx. \end{aligned} \tag{3.5}$$

We sum the variational formulations given by (3.2) over all elements to arrive at the global form of the two-dimensional UWLDG scheme:

$$\big((u_h)_t, p\big) - \alpha(w_h, p) + \beta\mathcal{B}(w_h, p) + (\widetilde{f}(u_h), p) = 0, \tag{3.6a}$$
$$(w_h, q) + \alpha(u_h, q) - \beta\mathcal{B}(u_h, q) = 0, \tag{3.6b}$$

where we have omitted the subscript Ω_h from the inner product notation $(\cdot,\cdot)_{\Omega_h}$ for brevity, and denoted the bilinear form $\mathcal{B}(\cdot,\cdot)$ as the sum over all elements, that is, $\mathcal{B}(\cdot,\cdot) := \sum_{K\in\Omega_h} \mathcal{B}_K(\cdot,\cdot)$.

3.3 Energy stability of the UWLDG scheme in 2D

In this subsection, we show the energy stability of the UWLDG method with the fluxes given in Table 3.1. To do that, we first establish the following lemma.

Lemma 3.1. *If the boundary conditions* (1.3a)-(1.3d) *are homogeneous, then*

(i) *For the G-Dirichlet B.C., Neumann B.C. and mixed B.C., we have*

$$\sum_{K\in\Omega_h} \mathcal{H}_{\partial K}\big((u_h)_t, w_h\big) = 0. \tag{3.7}$$

(ii) *For the Dirichlet B.C., we have*

$$\sum_{K\in\Omega_h} \mathcal{H}_{\partial K}\big((u_h)_t, w_h\big) = \frac{1}{2}\frac{d}{dt}\mathcal{S}\big(u_h\big). \tag{3.8}$$

Proof. For the proof of this lemma, we refer the reader to the proof of Lemma 3.2 in [18]. Since the techniques are very similar, we omit the details here to save space. □

Theorem 3.2. *For the two-dimensional EFK problem* (1.1) *with the homogeneous boundary conditions in* (1.3a)–(1.3d)*, the UWLDG solutions u_h, w_h of the scheme* (3.2) *with the numerical flux given in Table 3.1, satisfy the following stability:*

(i) *For the G-Dirichlet B.C., Neumann B.C. and mixed B.C., we have*

$$\frac{d}{dt}\int_{\Omega_h}\left(\frac{1}{2}(w_h(t))^2 + \widetilde{F}(u_h)\right)dx \le 0; \tag{3.9}$$

(ii) *For the Dirichlet B.C., we have*

$$\frac{d}{dt}\int_{\Omega_h}\left(\frac{1}{2}(w_h(t))^2 + \widetilde{F}(u_h) + \frac{\beta}{2}\mathcal{S}(u_h)\right)dx \le 0, \tag{3.10}$$

where $\widetilde{F}(u_h) = \frac{1}{4}\left((u_h)^2 - \left(1+\frac{1}{4\gamma}\right)\right)^2$ *and* $\mathcal{S}(u_h)$ *is determined by* (3.5).

Proof. Similarly to the one-dimensional case, we begin by taking the time derivative of the second equation in the scheme (3.6). Then, we choose test functions $p = (u_h)_t, q = w_h$ and add the two equations to obtain

$$\big((u_h)_t, (u_h)_t\big) + \big((w_h)_t, w_h\big) + \beta\Big(\mathcal{B}\big(w_h, (u_h)_t\big) - \mathcal{B}\big((u_h)_t, w_h\big)\Big) + \big(\widetilde{f}(u_h), (u_h)_t\big) = 0. \tag{3.11}$$

Using integration by parts, we derive

$$\mathcal{B}\big(w_h,(u_h)_t\big)-\mathcal{B}\big((u_h)_t,w_h\big)=\sum_{K\in\Omega_h}\mathcal{H}_{\partial K}\big((u_h)_t,w_h\big), \tag{3.12}$$

where $\mathcal{H}_{\partial K}(\cdot,\cdot)$ is defined by (3.4). Notice that

$$\big(\widetilde{f}(u_h),(u_h)_t\big)=\frac{d}{dt}\int_{\Omega_h}\widetilde{F}(u_h)dx,$$

then by combining (3.12) with (3.11), we arrive at

$$\frac{d}{dt}\int_{\Omega_h}\left(\frac{1}{2}(w_h(t))^2+\widetilde{F}(u_h)\right)dx+\|(u_h)_t\|^2+\beta\sum_{K\in\Omega_h}\mathcal{H}_{\partial K}\big((u_h)_t,w_h\big)=0.$$

By Lemma 3.1, we immediately obtain the stability (3.9) and (3.10), respectively. □

3.4 Optimal error estimates

This subsection focuses on the derivation of optimal error estimates of the UWLDG scheme (3.2) for the two-dimensional problem (1.1). Similar to the one-dimensional case, we primarily consider the G-Dirichlet B.C. (1.3a), and will provide remarks on how to extend these results to the other three boundary conditions. We begin by introducing some preliminaries and projections that are essential for our analysis.

3.4.1 Preliminaries and projections

We first introduce two semi-norms on the boundary of element $K=K_{ij}$ as follows.

$$\|v\|_{\partial K}:=\Big(\|v(x,y_{j-\frac{1}{2}})\|_{I_i}^2+\|v(x,y_{j+\frac{1}{2}})\|_{I_i}^2+\|v(x_{i-\frac{1}{2}},y)\|_{J_j}^2+\|v(x_{i+\frac{1}{2}},y)\|_{J_j}^2\Big)^{\frac{1}{2}},$$

$$\|v\|_{\ell,\partial K}:=\Big(\|v(x,y_{j-\frac{1}{2}})\|_{\ell,I_i}^2+\|v(x,y_{j+\frac{1}{2}})\|_{\ell,I_i}^2+\|v(x_{i-\frac{1}{2}},y)\|_{\ell,J_j}^2+\|v(x_{i+\frac{1}{2}},y)\|_{\ell,J_j}^2\Big)^{\frac{1}{2}}.$$

Then, we denote $\|\nabla v\|_{\partial K}=\big(\|v_x\|_{\partial K}^2+\|v_y\|_{\partial K}^2\big)^{\frac{1}{2}}$ and for any subset $\widetilde{K}\subseteq\Omega_h$,

$$\|v\|_{\partial\widetilde{K}}=\Big(\sum_{K\in\widetilde{K}}\|v\|_{\partial K}^2\Big)^{\frac{1}{2}},\quad \|\nabla v\|_{\partial\widetilde{K}}=\Big(\sum_{K\in\widetilde{K}}\|\nabla v\|_{\partial K}^2\Big)^{\frac{1}{2}},\quad \|v\|_{\ell,\widetilde{K}}=\Big(\sum_{K\in\widetilde{K}}\|v\|_{\ell,K}^2\Big)^{\frac{1}{2}}.$$

The following two-dimensional version trace and inverse inequalities [15, 4] are useful in our subsequent analysis.

Lemma 3.3. *For any $v\in H^1(K)$, there exists a positive constant C, such that*

$$\|v\|_{\partial K}^2\le C\|v\|_K\|v\|_{1,K},$$

where C is independent of the mesh size h.

Lemma 3.4. *For any $q \in \mathcal{Q}^k(K)$, there exist a positive constants C, such that*

$$\|q\|_{\partial K} \le C h_K^{-\frac{1}{2}} \|q\|_K, \quad \|\nabla q\|_K \le C h_K^{-1} \|q\|_K, \quad \|q\|_\infty \le C h^{-1} \|q\|,$$

where C is independent of the mesh size h.

Next, for two-dimensional Cartesian meshes, we construct the projection as the tensor product of one-dimensional projections. We define $\Pi : H^2(\Omega_h) \to W_h$ as

$$\Pi u := \mathbb{P}_{\mathrm{I}_x} \otimes \mathbb{P}_{\mathrm{I}_y} u\,, \tag{3.13}$$

where $\mathbb{P}_{\mathrm{I}}$ is the one-dimensional projection given by (2.22a), and the subscripts x and y indicate the application of the one-dimensional operator $\mathbb{P}_{\mathrm{I}}$ with respect to the x-direction and y-direction, respectively. Specifically, Πu satisfies:

$$\Pi u|_{K_{11}} = (\mathsf{P}_3|_{I_1} \otimes \mathsf{P}_3|_{J_1})u, \tag{3.14a}$$
$$\Pi u|_{K_{1j}} = (\mathsf{P}_3|_{I_1} \otimes \mathsf{P}_1|_{J_j})u,\ j = 2, 3, \ldots, N, \tag{3.14b}$$
$$\Pi u|_{K_{i1}} = (\mathsf{P}_1|_{I_i} \otimes \mathsf{P}_3|_{J_1})u,\ i = 2, 3, \ldots, N, \tag{3.14c}$$
$$\Pi u|_{K_{ij}} = (\mathsf{P}_1|_{I_i} \otimes \mathsf{P}_1|_{J_j})u,\ i, j = 2, 3, \ldots, N. \tag{3.14d}$$

The existence and uniqueness of the projection Π is easy to show by using an argument similar to that in [30, Lemma 6.1], and thus the proof is omitted. We also have the following approximation property.

Lemma 3.5. *Assume that $u \in H^s(\Omega_h)$, $s \ge 2$, then there exists a unique $\Pi u \in W_h$ satisfying* (3.13)*. Moreover, there holds*

$$\|u - \Pi u\|_K + h^\ell \|u - \Pi u\|_{\ell,K} + h^{\frac{1}{2}} \|u - \Pi u\|_{\partial K} \le C h^{min\{k+1,\ s\}} \|u\|_{s,K},$$

where $1 \le \ell \le min\{k+1,\ s\}$ is an integer and C is a constant independent of h.

3.4.2 Error estimates

Theorem 3.6. *Let u be the exact solution of the EFK equation* (1.1) *with the G-Dirichlet B.C.* (1.3a)*, $w = -\alpha u + \beta \Delta u$. Assume $\|u\|_{k+5}$, $\|u_t\|_{k+1}$ are bounded uniformly for any time t and $k > 1$. Let u_h, w_h be solutions of the UWLDG scheme* (3.2) *with the numerical flux given in Table 3.1, then we have*

$$\|u(t) - u_h(t)\| + \int_0^t \|w(\tau) - w_h(\tau)\|\, d\tau \le C h^{k+1}, \tag{3.15}$$

where C is a constant independent of h and dependent on $\|u\|_{k+5}$, $\|u_t\|_{k+1}$, and t.

The proof of Theorem 3.6 is provided in the following subsection.

Remark 3.7. *When $k = 1$, the boundary flux for the G-Dirichlet B.C. in Table 3.1 cannot be constructed due to the non-existence of the projection $\mathbb{P}_{\mathrm{I}}$, and hence we require $k > 1$ in Theorem 3.6. Numerically, when $k = 1$, if we directly use the actual boundary information to construct the boundary numerical flux, our numerical experiments reveal that only half-order accuracy is achieved for both the L^2 errors $\|e_u\|$ and $\|e_w\|$; see Tables 4.3 and 4.4 in Section 4, respectively.*

Remark 3.8. *For the other three kinds of boundary conditions, we can prove that for $k \geq 1$, the corresponding UWLDG solutions satisfy the optimal error estimate result given by* (3.15) *by employing a similar proof strategy as in Theorem 3.6. It is worth pointing out that, in the analysis of error estimates, the projections should be chosen as $\mathbb{P}_{\mathrm{II}_x} \otimes \mathbb{P}_{\mathrm{II}_y}$ for cases of Dirichlet B.C. and the mixed B.C., respectively; and $\mathbb{P}_{\mathrm{III}_x} \otimes \mathbb{P}_{\mathrm{III}_y}$ for the case of Neumann B.C. In particular, for the Dirichlet B.C. case, we refer to [18] for a detailed technical analysis of the error terms arising from penalty terms in the proof of error estimates.*

3.4.3 The Proof of error estimates

In this section, we present the proof of Theorem 3.6, which are shown in the following six steps:
Step 1. Error equation. Denote

$$e_u = u - u_h, \quad e_w = w - w_h.$$

Since the exact solutions u and w satisfy the following weak formulation:

$$\begin{aligned}(u_t, p)_K - \alpha(w, p)_K + \beta\big((w, \Delta p)_K + \langle \nabla w \cdot \mathbf{n}, p\rangle_{\partial K} - \langle w, \nabla p \cdot \mathbf{n}\rangle_{\partial K}\big) + \big(\widetilde{f}(u), p\big) = 0,\\ (w, q)_K + \alpha(u, q) - \beta\big((u, \Delta q)_K + \langle \nabla u \cdot \mathbf{n}, q\rangle_{\partial K} - \langle u, \nabla q \cdot \mathbf{n}\rangle_{\partial K}\big) = 0,\end{aligned}$$

then we can get the cell error equation as

$$\big((e_u)_t, p\big)_K - \alpha(e_w, p)_K + \beta\mathcal{B}_K\big(e_w, p\big) + \big(\widetilde{f}(u) - \widetilde{f}(u_h), p\big) = 0, \tag{3.16a}$$

$$(e_w, q)_K + \alpha(e_u, q)_K - \beta\mathcal{B}_K\big(e_u, q\big) = 0, \tag{3.16b}$$

where $\mathcal{B}_K(\cdot,\cdot)$ is defined by (3.3), and

$$\widehat{e_u} = u - \widehat{u_h}, \quad \widehat{\nabla e_u} \cdot \mathbf{n} = (\nabla u - \widehat{\nabla u_h}) \cdot \mathbf{n}, \quad \widehat{e_w} = w - \widehat{w_h}, \quad \widehat{\nabla e_w} \cdot \mathbf{n} = (\nabla w - \widehat{\nabla w_h}) \cdot \mathbf{n}.$$

Step 2. Error decomposition. Denote $e_u = \eta_u - \xi_u$, $e_w = \eta_w - \xi_w$ with

$$\eta_u = u - \Pi u,\ \xi_u = u_h - \Pi u, \quad \eta_w = w - \Pi w,\ \xi_w = w_h - \Pi w.$$

According to the G-Dirichlet B.C. (1.3a) and the associated boundary flux in Table 3.1, we let

$$\widehat{\eta_u}\big|_e := \widehat{e_u}\big|_e, \qquad \widehat{\eta_w}\big|_e := \widehat{e_w}\big|_e, \quad \forall e \in \mathscr{E}_h^0, \tag{3.17a}$$

and

$$\widehat{\xi_u}\big|_e := 0, \qquad \widehat{\xi_w}\big|_e := 0, \quad \forall e \in \mathscr{E}_h^0. \tag{3.17b}$$

Then, we decompose the cell error equation (3.16) into the following form

$$\begin{aligned}\big((\xi_u)_t, p\big)_K - \alpha(\xi_w, p)_K + \beta\mathcal{B}_K\left(\xi_w, p\right) &= \big((\eta_u)_t, p\big)_K - \alpha(\eta_w, p)_K + \beta\mathcal{B}_K\left(\eta_w, p\right)\\ &\quad + \big(\widetilde{f}(u) - \widetilde{f}(u_h), p\big)_K,\\ (\xi_w, q)_K + \alpha(\xi_u, q)_K - \beta\mathcal{B}_K\left(\xi_u, q\right) &= (\eta_w, q)_K + \alpha(\eta_u, q)_K - \beta\mathcal{B}_K\left(\eta_u, q\right).\end{aligned} \tag{3.18}$$

Now, let us take test functions $p = \xi_u$ and $q = \xi_w$. By adding the two equations in (3.18) and summing over all K, we obtain

$$\begin{aligned}\big((\xi_u)_t, \xi_u\big) + (\xi_w, \xi_w) + \beta\Theta_1 = \big((\eta_u)_t, \xi_u\big) + (\eta_w, \xi_w) + \alpha(\eta_u, \xi_w) - \alpha(\eta_w, \xi_u) \\ + \beta\Theta_2 + \big(\widetilde{f}(u) - \widetilde{f}(u_h), \xi_u\big),\end{aligned} \tag{3.19}$$

where

$$\Theta_1 = \mathcal{B}(\xi_w, \xi_u) - \mathcal{B}(\xi_u, \xi_w), \quad \Theta_2 = \mathcal{B}(\eta_w, \xi_u) - \mathcal{B}(\eta_u, \xi_w). \tag{3.20}$$

Step 3. The estimate of Θ_1. The estimate of Θ_1 is given in the following lemma.

Lemma 3.9. *For Θ_1 defined in (3.20), we have*

$$\Theta_1 = \sum_{K\in\Omega_h} \Big(\mathcal{B}_K(\xi_w, \xi_u) - \mathcal{B}_K(\xi_u, \xi_w)\Big) = 0. \tag{3.21}$$

Proof. By the property of $\mathcal{B}$ as in (3.12), the boundary flux (3.17b) and Lemma 3.1, we can directly obtain (3.21). □

Step 4. The estimate of Θ_2.

The following lemma shows that projection error terms have polynomial preserving properties up to degree $k+2$, which is crucial for estimating Θ_2.

Lemma 3.10. *If $w, u \in \mathcal{P}^{k+2}$ $(k > 1)$, $p, q \in W_h$, we have*

$$\mathcal{B}_K(\eta_w, p) = 0, \quad \forall K \in \Omega_h, \tag{3.22a}$$

$$\mathcal{B}_K(\eta_u, q) = 0, \quad \forall K \in \Omega_h. \tag{3.22b}$$

Proof. Since the projection Π is polynomial preserving up to degree k, then (3.22) holds when $w, u \in \mathcal{Q}^k(K)$. Hence, we only need to consider the following six cases

$$x^{k+2}, \quad y^{k+2}, \quad x^{k+1}y, \quad xy^{k+1}, \quad x^{k+1}, \quad y^{k+1}. \tag{3.23}$$

The detailed proof is similar to that of [18, Lemma 3.11], and we need only to pay special attention to the expressions of $B_K(\eta_w, q)$ and $B_K(\eta_u, q)$ on the boundary elements. Therefore, we omit it here. □

By Lemma 3.10, we can establish a superconvergent property for $\mathcal{B}_K(\eta_w, p)$ and $\mathcal{B}_K(\eta_u, q)$, as given in Lemma 3.11.

Lemma 3.11. *For $p, q \in W_h$ and $k > 1$, we have*

$$\sum_{K\in\Omega_h} |\mathcal{B}_K(\eta_w, p)| \le Ch^{k+1}\|w\|_{k+3}\|p\|, \tag{3.24a}$$

$$\sum_{K\in\Omega_h} |\mathcal{B}_K(\eta_u, q)| \le Ch^{k+1}\|u\|_{k+3}\|q\|, \tag{3.24b}$$

where C is a constant independent of the mesh size h.

Proof. The proof of this lemma is provided in Appendix A.2. □

Taking $p = \xi_u$, $q = \xi_w$ in Lemma 3.11, we can immediately get the estimate of Θ_2 in the following Lemma 3.12.

Lemma 3.12. *For Θ_2 defined in* (3.20)*, we have*

$$|\Theta_2| \le Ch^{k+1}\|\xi_u\| + Ch^{k+1}\|\xi_w\|, \tag{3.25}$$

where C depends on $\|u\|_{k+5}$, but is independent of the mesh size h.

Step 5. The estimate of $(\widetilde{f}(u) - \widetilde{f}(u_h), \xi_u)$. For the two-dimensional case, the estimates of $(\widetilde{f}(u) - \widetilde{f}(u_h), \xi_u)$ can be derived using a similar approach to that employed in the proof of (2.30) for the one-dimensional case in Section 2.3.2, and the main difference is that we now have

$$\|\xi_u\|_\infty \le Ch^{-1}\|\xi_u\|, \quad \|\eta_u\|_\infty \le Ch^k\|u\|_{k+1}, \tag{3.26}$$

which is obtained by the inverse inequality in Lemma 3.4 and the scaling argument. Therefore, for the two-dimensional case, we obtain

$$\left|\left(\widetilde{f}(u) - \widetilde{f}(u_h), \xi_u\right)\right| \le C\|\xi_u\|^2 + Ch^{-2}\|\xi_u\|^4 + Ch^{2k+2}. \tag{3.27}$$

Step 6. The final proof of Theorem 3.6.

Now, we are ready to give the last part of the proof. Recalling the error equation (3.19), and using the Cauchy–Schwarz inequality and approximation property of the projection Π in Lemma 3.5, we arrive at

$$\frac{1}{2}\frac{d}{dt}\|\xi_u(t)\|^2 + \|\xi_w(t)\|^2 + \beta\Theta_1 \le Ch^{k+1}\|\xi_u(t)\| + Ch^{k+1}\|\xi_w(t)\| + \beta|\Theta_2| + \left|(\widetilde{f}(u) - \widetilde{f}(u_h), \xi_u)\right|.$$

By Lemma 3.9, Lemma 3.12 and (3.27), we have

$$\frac{1}{2}\frac{d}{dt}\|\xi_u\|^2 + \frac{1}{2}\|\xi_w\|^2 \le C\|\xi_u\|^2 + Ch^{-2}\|\xi_u\|^4 + Ch^{2k+2}. \tag{3.28}$$

Now, using Lemma 2.4, we immediately obtain

$$\|\xi_u\| \le Ch^{k+1}. \tag{3.29}$$

Combining (3.28) and (3.29), and integrating with respect to t, we have

$$\|\xi_u(t)\| + \int_0^t \|\xi_w(\tau)\|\, d\tau \le Ch^{k+1},$$

and hence

$$\|e_u(t)\| + \int_0^t \|e_w(\tau)\|\, d\tau \le Ch^{k+1},$$

where C depends on $\|u\|_{k+5}$, $\|u_t\|_{k+1}$ and t, but is independent of h.

4 Numerical examples

In this section, three examples are presented to confirm the theoretical results and to demonstrate effectiveness of the proposed UWLDG method. Examples 4.1 and 4.3 are benchmark examples used to verify the accuracy for one- and two-dimensional EFK problems, respectively. Example 4.2 investigates the effective simulation and approximation of the EFK problem in cases where no analytical solution is available. In all experiments, the four-stage third-order implicit explicit Runge–Kutta method is adopted for time discretization, and all numerical tests are performed on uniform meshes.

Example 4.1. *Consider the one-dimensional EFK equation*

$$u_t + \gamma u_{xxxx} - u_{xx} + u^3 - u = g(x,t), \quad (x,t) \in [0, 0.5] \times (0, T],$$

with the initial condition

$$u(x,0) = \sin(\pi x),$$

and boundary conditions as described in (1.3a)–(1.3d)*. The exact solution and the source term are given as follows:*

$$u(x,t) = e^{-t}\sin(\pi x),$$

$$g(x,t) = e^{-3t}\sin^3(\pi x) + e^{-t}(-2 + \pi^2 + \pi^4)\sin(\pi x).$$

For the G-Dirichlet, Dirichlet, Neumann and mixed boundary conditions, our computations are based on the flux selections detailed in (2.6)-(2.9). The errors $\|e_u\|$, $\|e_w\|$ and the accuracy orders for $1 \le k \le 3$ are presented in Tables 4.1 and 4.2, respectively. These tables illustrate the expected optimal $(k+1)$th order, with the exception of the G-Dirichlet B.C. case when using $\mathcal{P}^1$ polynomials. This confirms the theoretical findings shown in Theorem 2.5 and discussions in Remarks 2.6 and 2.7.

Example 4.2. *In this particular example, we test the one-dimensional EFK problem*

$$u_t + \gamma u_{xxxx} - u_{xx} + u^3 - u = 0, \quad (x,t) \in [-4,\ 4] \times (0, T],$$

with initial condition

$$u(x,0) = 0.001e^{-x^2},$$

and boundary conditions :

$$u(-4,t) = 1,\ u(4,t) = 1, \quad u_{xx}(-4,t) = 0,\ u_{xx}(4,t) = 0.$$

For this problem, the analytical solution is unknown. This example was first studied in [10] to demonstrate the physical behavior of the EFK equation with a small parameter γ. To illustrate effectiveness of our UWLDG method, we take $\gamma = 0.0001$ to calculate the numerical solutions at $T = 0.25,\ 1.0,\ 1.75,\ 2.5\ , 3.5,\ 4.5$. The time evolution of the semi-discrete solutions are shown in Figure 4.1. It illustrates that as time increases, the UWLDG solution of u gradually converges to the value 1, which represents the stable state of the EFK equation. This result exhibits the same patterns as those presented in [3, 10].

Table 4.1: L^2 errors and orders of u for Example 4.1 with the G-Dirichlet, Dirichlet, Neumann and mixed boundary conditions using $\mathcal{P}^k$ polynomials on a uniform mesh of N cells, $T = 1$; $\gamma = 1$.

	N	G-Dirichlet B.C.		Dirichlet B.C.		Neumann B.C.		mixed B.C.	
		$\|e_u\|$	Order	$\|e_u\|$	Order	$\|e_u\|$	Order	$\|e_u\|$	Order
$\mathcal{P}^1$	20	3.27E-01	–	5.92E-04	–	4.70E-04	–	8.36E-04	–
	40	1.96E-01	0.74	1.47E-04	2.00	1.24E-04	1.91	2.08E-04	2.00
	80	1.03E-01	0.92	3.69E-05	2.00	3.20E-05	1.95	5.21E-05	2.00
	160	4.46E-02	1.21	9.24E-06	1.99	8.11E-06	1.98	1.30E-05	2.00
	320	1.68E-02	1.40	2.31E-06	1.99	2.04E-06	1.99	3.25E-06	2.00
	640	6.07E-03	1.47	5.79E-07	1.99	5.12E-07	1.99	8.14E-07	2.00
$\mathcal{P}^2$	20	1.85E-06	–	1.53E-06	–	1.53E-06	–	1.53E-06	–
	40	2.13E-07	3.12	1.92E-07	2.99	1.92E-07	2.99	1.92E-07	2.99
	80	2.53E-08	3.07	2.40E-08	2.99	2.40E-08	2.99	2.40E-08	2.99
	160	3.09E-09	3.03	3.00E-09	2.99	3.01E-09	2.99	3.00E-09	2.99
	320	3.81E-10	3.01	3.75E-10	2.99	3.77E-10	2.99	3.75E-10	3.00
$\mathcal{P}^3$	10	8.63E-08	–	8.62E-08	–	8.07E-08	–	8.62E-08	–
	20	5.38E-09	4.00	5.38E-09	4.00	5.21E-09	3.95	5.38E-09	4.00
	40	3.36E-10	4.00	3.36E-10	4.00	3.30E-10	3.97	3.36E-10	4.00
	80	2.09E-11	4.00	2.09E-11	4.00	2.08E-11	3.98	2.09E-11	4.00
	160	1.31E-12	4.00	1.31E-12	4.00	1.30E-12	3.99	1.21E-12	4.00

Table 4.2: L^2 errors and orders of w for Example 4.1 with the G-Dirichlet, Dirichlet, Neumann and mixed boundary conditions using $\mathcal{P}^k$ polynomials on a uniform mesh of N cells, $T = 1$; $\gamma = 1$.

	N	G-Dirichlet B.C.		Dirichlet B.C.		Neumann B.C.		mixed B.C.	
		$\|e_w\|$	Order	$\|e_w\|$	Order	$\|e_w\|$	Order	$\|e_w\|$	Order
$\mathcal{P}^1$	20	1.32E-01	–	2.48E-03	–	3.39E-03	–	6.12E-03	–
	40	8.67E-02	0.60	6.32E-04	1.97	8.63E-04	1.97	1.52E-03	2.00
	80	4.77E-02	0.86	1.60E-04	1.98	2.18E-04	1.98	3.82E-04	2.00
	160	2.09E-02	1.19	4.04E-05	1.98	5.48E-05	1.99	9.61E-05	2.00
	320	7.93E-03	1.39	1.02E-05	1.98	1.37E-05	1.99	2.42E-05	2.00
	640	2.86E-03	1.47	2.59E-06	1.99	3.43E-06	2.00	6.09E-06	1.99
$\mathcal{P}^2$	20	1.92E-05	–	1.59E-05	–	1.59E-05	–	1.59E-05	–
	40	2.21E-06	3.12	1.99E-06	2.99	2.00E-06	2.99	1.99E-06	2.99
	80	2.63E-07	3.07	2.49E-07	2.99	2.56E-07	2.97	2.49E-07	2.99
	160	3.20E-08	3.03	3.11E-08	3.00	3.24E-08	2.98	3.11E-09	3.00
	320	3.95E-09	3.01	3.89E-09	3.00	4.07E-09	2.99	3.89E-09	3.00
$\mathcal{P}^3$	10	8.96E-07	–	8.96E-07	–	8.37E-07	–	8.95E-07	–
	20	5.59E-08	4.00	5.60E-08	4.00	5.40E-08	3.95	5.59E-08	4.00
	40	3.50E-09	4.00	3.52E-09	4.00	3.43E-09	3.97	3.50E-09	4.00
	80	2.20E-10	4.00	2.23E-10	3.98	2.16E-10	3.98	2.20E-10	4.00
	160	1.40E-11	3.97	1.45E-11	3.94	1.35E-11	3.99	1.40E-11	3.98

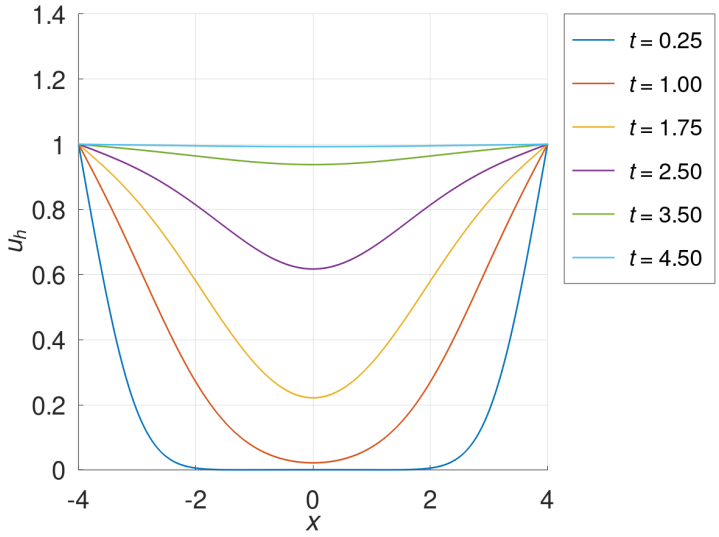

Figure 4.1: The profile of u_h; $\gamma = 0.0001$.

Example 4.3. *Consider the following two-dimensional EFK problem*

$$u_t + \gamma\Delta^2 u - \Delta u + u^3 - u = g(x, y, t), \qquad (x, y) \in [0, 2\pi] \times [0, 2\pi],\ t \in (0, T],$$

with the initial condition

$$u(x, y, 0) = \sin(x + y),$$

and the source term

$$g(x, y, t) = (4\gamma - 3)e^{-4t}\sin(x + y) + e^{-12t}\sin^3(x + y),$$

equipped with boundary conditions (1.3a)–(1.3d) *such that the exact solution is*

$$u(x, y, t) = e^{-4t}\sin(x + y).$$

Table 4.3 and Table 4.4 show the L^2 errors $\|e_u\|$, $\|e_w\|$, and orders for Example 4.3 with G-Dirichlet, Dirichlet, Neumann, and mixed boundary conditions using $\mathcal{Q}^k$ polynomials, where $1 \le k \le 3$. We would like to point out that for the G-Dirichlet boundary conditions with $\mathcal{Q}^1$ polynomials, the exact boundary conditions were used to define the boundary numerical fluxes $\widehat{u}$ and $\widehat{w}$, That is, $\widehat{u}|e = f_D|e$ and $\widehat{w}|e = \widetilde{g}_D|e$. This approach was necessary because the projection $\mathbb{P}_1$ does not exist when $k = 1$, and thus the construction of the numerical flux as described in Table 3.1 cannot be achieved. Numerical results demonstrate that approximately one and a half orders are lost for both $\|e_u\|$ and $\|e_w\|$.

These observations align with the theoretical findings detailed in Theorem 3.6 and Remarks 3.7–3.8. The results show that optimal order can be achieved, except when the G-Dirichlet boundary conditions are considered with $\mathcal{Q}^1$ polynomials, for which we observe a reduction of order.

Table 4.3: L^2 errors and orders of u for Example 4.3 with the G-Dirichlet, Dirichlet, Neumann and mixed boundary conditions using $\mathcal{Q}^k$ polynomials on a uniform mesh of $N \times N$ cells, $T = 1$; $\gamma = 1$.

	$N \times N$	G-Dirichlet B.C.		Dirichlet B.C.		Neumann B.C.		mixed B.C.	
		$\|e_u\|$	Order	$\|e_u\|$	Order	$\|e_u\|$	Order	$\|e_u\|$	Order
	10×10	1.24E-01	–	7.17E-03	–	1.41E-02	–	1.55E-02	–
	20×20	8.13E-02	0.61	1.84E-03	1.95	2.98E-02	2.23	3.69E-03	2.07
$\mathcal{Q}^1$	40×40	5.60E-02	0.53	4.74E-04	1.96	6.89E-02	2.11	9.23E-04	2.00
	60×60	4.73E-02	0.41	2.12E-04	1.98	3.00E-02	2.04	4.09E-04	2.00
	80×80	3.94E-02	0.62	1.19E-04	1.98	1.67E-02	2.02	2.30E-04	2.00
	10×10	7.50E-05	–	9.50E-05	–	5.99E-05	–	7.56E-05	–
	20×20	7.96E-06	3.23	7.27E-06	3.70	7.03E-06	3.09	7.28E-06	3.37
$\mathcal{Q}^2$	40×40	9.31E-07	3.09	8.81E-07	3.04	8.72E-07	3.01	8.85E-07	3.04
	60×60	2.70E-07	3.05	2.60E-07	3.00	2.58E-07	2.99	2.60E-07	3.01
	80×80	1.12E-07	3.03	1.09E-07	3.00	1.07E-07	2.99	1.09E-07	3.00
	10×10	1.70E-06	–	3.74E-06	–	1.50E-06	–	1.56E-06	–
	15×15	3.27E-07	4.06	3.68E-07	5.71	3.01E-07	3.96	3.08E-07	3.99
$\mathcal{Q}^3$	20×20	1.02E-07	4.04	1.00E-07	4.52	9.61E-08	3.97	9.77E-08	3.99
	25×25	4.15E-08	4.03	3.99E-08	4.11	3.95E-08	3.98	4.00E-08	3.99
	30×30	1.99E-08	4.03	1.92E-08	4.02	1.91E-08	3.98	1.93E-08	3.99

Table 4.4: L^2 errors and orders of w for Example 4.3 with the G-Dirichlet, Dirichlet, Neumann and mixed boundary conditions using $\mathcal{Q}^k$ polynomials on a uniform mesh of $N \times N$ cells, $T = 1$; $\gamma = 1$.

	$N \times N$	G-Dirichlet B.C.		Dirichlet B.C.		Neumann B.C.		mixed B.C.	
		$\|e_w\|$	Order	$\|e_w\|$	Order	$\|e_w\|$	Order	$\|e_w\|$	Order
	10×10	1.18E-01	–	1.29E-02	–	1.98E-02	–	1.73E-02	–
	20×20	1.07E-01	0.14	3.75E-03	1.79	4.55E-03	2.12	4.23E-03	2.02
$\mathcal{Q}^1$	40×40	7.97E-02	0.43	9.74E-04	1.95	1.12E-03	2.01	1.07E-03	1.98
	60×60	6.59E-02	0.47	4.36E-04	1.98	5.01E-04	2.00	4.80E-04	1.99
	80×80	5.70E-02	0.50	2.46E-04	1.99	2.82E-04	2.00	2.70E-04	2.00
	10×10	1.82E-04	–	1.99E-04	–	1.44E-04	–	1.46E-04	–
	20×20	1.99E-05	3.19	1.95E-05	3.35	1.74E-05	3.05	1.77E-05	3.05
$\mathcal{Q}^2$	40×40	2.34E-06	3.09	2.25E-06	3.11	2.17E-06	3.00	2.19E-06	3.01
	60×60	6.79E-07	3.05	6.57E-07	3.03	6.45E-07	2.99	6.49E-07	3.00
	80×80	2.83E-07	3.03	2.77E-07	3.00	2.73E-07	2.99	2.74E-07	3.00
	10×10	1.70E-06	–	3.74E-06	–	1.50E-06	–	1.56E-06	–
	15×15	3.27E-07	4.06	3.68E-07	5.71	3.01E-07	3.96	3.08E-07	3.99
$\mathcal{Q}^3$	20×20	1.02E-07	4.04	1.00E-07	4.52	9.61E-08	3.97	9.77E-08	3.99
	25×25	4.15E-08	4.03	3.99E-08	4.11	3.95E-08	3.98	4.00E-08	3.99
	30×30	1.99E-08	4.03	1.92E-08	4.02	1.91E-08	3.98	1.93E-08	3.99

5 Concluding remarks

As an extension and application of the results in [18] for the linear fourth-order initial boundary problem, this paper is devoted to analyzing the UWLDG method for the EFK problem under four types of typical boundary conditions. This method is proved to be energy stable for both one- and two-dimensional EFK problems, achieving this by designing alternating numerical fluxes for interior faces and imposing proper penalty terms on boundary faces when necessary. The optimal error estimates are obtained by appropriately constructing projections that match different boundary conditions. These theoretical results are numerically validated through experiments conducted on Cartesian meshes for one- and two-dimensional EFK examples. A one-dimensional EFK problem with a small parameter is also tested, confirming the validity and robustness of our method. Future work includes the analysis of optimal error estimates on triangular meshes for multi-dimensional EFK problems.

Appendix A Proof of a few technical lemmas

A.1 Proof of Lemma 2.4

Proof. We denote

$$L(t) = h^{2k+2} + \int_0^t h^{-2}s^2(\tau) + s(\tau)d\tau.$$

Since $s'(t) \le C(h^{-2}s^2 + s + h^{2k+2})$, $s(0) \le Ch^{2k+2}$, we integrate over $(0,t)$ to obtain

$$\begin{aligned} s(t) &\le s(0) + \int_0^t C\big(h^{-2}s^2(\tau) + s(\tau) + h^{2k+2}\big)\,d\tau \\ &\le Ch^{2k+2} + C\int_0^t h^{-2}s^2(\tau) + s(\tau)\,d\tau + Cth^{2k+2} \\ &\le CL(t) + CTL(t) = C(T+1)L(t), \end{aligned}$$

and hence

$$L'(t) = h^{-2}s^2(t) + s(t) \le C^\star\Big(h^{-2}L^2(t) + L(t)\Big),$$

where $C^\star = \max\{C^2(T+1)^2, C(T+1)\}$. Therefore,

$$\int_0^t \frac{L'(\tau)}{h^{-2}L^2(\tau) + L(\tau)}d\tau \le C^\star T,$$

and

$$\begin{aligned} \mathcal{F}\Big(\frac{L(t)}{L(0)}\Big) &:= \int_1^{\frac{L(t)}{L(0)}} \frac{1}{y + h^{2k}y^2}dy \\ &= \int_1^{\frac{L(t)}{L(0)}} \frac{1}{y + h^{-2}y^2L(0)}dy = \int_0^t \frac{L'(\tau)}{h^{-2}L^2(\tau) + L(\tau)}d\tau \le C^\star T. \end{aligned}$$

It is easy to check $\mathcal{F}(\omega) = \ln\big(\frac{\omega}{1+h^{2k}\omega}\big) + \ln(1+h^{2k})$ and

$$\mathcal{F}\Big(\frac{2e^{C^\star T+1}}{1 - h^{2k}e^{C^\star T+1}}\Big) \ge C^\star T.$$

Denoting $C_1 = 4e^{C^\star T+1}$, we have $C_1 \geq \frac{2e^{C^\star T+1}}{1-h^{2k}e^{C^\star T+1}}$ as h small enough. Since $\mathcal{F}(\omega)$ is increasing with ω and hence

$$\mathcal{F}(C_1) \geq \mathcal{F}\Big(\frac{2e^{C^\star T+1}}{1-h^{2k}e^{C^\star T+1}}\Big) \geq C^\star T \geq \mathcal{F}\Big(\frac{L(t)}{L(0)}\Big),$$

then $\frac{L(t)}{L(0)} \leq C_1$, and

$$s(t) \leq C^\star L(t) \leq C^\star C_1 L(0) = \widetilde{C} h^{2k+2},$$

here, $\widetilde{C} = C^\star C_1$ is independent of h and dependent on T. □

A.2 Proof of Lemma 3.11

Proof. Without of loss of generality, we only show the proof of (3.24a). For easy presentation, $\forall\ \zeta \in H^2(\Omega_h)$, $p \in W_h$, $i=1,2,\ldots,N_x-1,\ j=1,2,\ldots,N_y-1$, we denote

$$\begin{aligned}
&T_0^{ij}(\zeta,p) = \int_{K_{ij}} \zeta\,(p_{xx}+p_{yy})\,dxdy,\\
&T_1^{ij}(\zeta,p) = -\int_{J_j} \zeta(x^+_{i+\frac12},y)\,p_x(x^-_{i+\frac12},y)\,dy, \quad T_2^{ij}(\zeta,p) = \int_{J_j} \zeta(x^+_{i-\frac12},y)\,p_x(x^+_{i-\frac12},y)\,dy,\\
&T_3^{ij}(\zeta,p) = -\int_{I_i} \zeta(x,y^+_{j+\frac12})\,p_y(x,y^-_{j+\frac12})\,dx, \quad T_4^{ij}(\zeta,p) = \int_{I_i} \zeta(x,y^+_{j-\frac12})\,p_y(x,y^+_{j-\frac12})\,dx,\\
&T_5^{ij}(\zeta,p) = \int_{J_j} \zeta_x(x^-_{i+\frac12},y)\,p(x^-_{i+\frac12},y)\,dy, \qquad T_6^{ij}(\zeta,p) = -\int_{J_j} \eta_x(x^-_{i-\frac12},y)\,p(x^+_{i-\frac12},y)\,dy,\\
&T_7^{ij}(\zeta,p) = \int_{I_i} \zeta_y(x,y^-_{j+\frac12})\,p(x,y^-_{j+\frac12})\,dx, \qquad T_8^{ij}(\zeta,p) = -\int_{I_i} \zeta_y(x,y^-_{j-\frac12})\,p(x,y^+_{j-\frac12})\,dx.
\end{aligned}$$

- $\boldsymbol{K \in \Omega_h^I}$.

Suppose $K = K_{ij}$, $i \in \{2,3,\ldots,N_x-1\}$, $j \in \{2,3,\ldots,N_y-1\}$. From the choice of the numerical flux at interior faces, we have: for any $v \in H^2(\Omega_h)$,

$$\mathcal{B}_K(\eta_v,p) = \mathcal{B}_{K_{ij}}(\eta_v,p) = \sum_{m=0}^{8} T_m^{ij}(\eta_v,p). \tag{A.1}$$

Since $k \geq 2$, by the Cauchy–Schwarz inequality, the approximation property of the projection Π, trace and inverse inequalities, we can establish the following rough estimate: for any $v \in H^3(\Omega_h)$ and $K \in \Omega_h^I$,

$$\begin{aligned}
\big|B_K(\eta_v,p)\big| &\leq \|\eta_v\|_K\|\Delta p\|_K + C\|\eta_v\|_{\partial\widetilde{K}}\|\nabla p\|_{\partial K} + C\|\nabla\eta_v\|_{\partial\widetilde{K}}\|p\|_{\partial K}\\
&\leq Ch^3\|v\|_{3,K}h^{-2}\|p\|_K + Ch^{\frac52}\|v\|_{3,\widetilde{K}}h^{-\frac32}\|p\|_K + Ch^{\frac32}\|v\|_{3,\widetilde{K}}h^{-\frac12}\|p\|_K\\
&\leq Ch\|v\|_{3,\widetilde{K}}\|p\|_K,
\end{aligned} \tag{A.2}$$

where $\widetilde{K} = \{K_{i+1,j},\ K_{i-1,j},\ K_{ij},\ K_{i,j-1},\ K_{i,j+1}\}$. Let χ be any polynomial of degree at most $k+2$, by (3.22a) in Lemma 3.10, we have

$$B_K(\eta_\chi,p) = 0,\ \forall p \in W_h.$$

Then, by the linearity of operator $B_K(\cdot,p)$ and the estimate (A.2), we get

$$B_K(\eta_w,p)=B_K(\eta_w,p)-B_K(\eta_\chi,p)=B_K(\eta_{w-\chi},p)\le Ch\|w-\chi\|_{3,\widetilde{K}}\|p\|_K.$$

Consequently,

$$\big|B_K(\eta_w,p)\big|\le Ch\inf_{\chi\in\mathcal{P}^{k+2}}\|w-\chi\|_{3,\widetilde{K}}\|p\|_K\le Ch^{k+1}\|w\|_{k+3,\widetilde{K}}\|p\|_K,\quad\forall K\in\Omega_h^I. \tag{A.3}$$

- $\boldsymbol{K\in\Omega_h^0}$. We take the element $K=K_{11}$ as an example, and we have

$$B_{K_{11}}(\eta_w,p)=B^T_{K_{11}}(\eta_w,p)+B^S_{K_{11}}(w,p),$$

where

$$\begin{aligned}B^T_{K_{11}}(\eta_w,p):=&\,T_0^{11}(\eta_w,p)+T_1^{11}(\eta_w,p)+T_3^{11}(\eta_w,p)+T_5^{11}(\eta_w,p)+T_7^{11}(\eta_w,p)\\&+\widetilde{T}_6^{11}(\eta_w,p)+\widetilde{T}_8^{11}(\eta_w,p),\\ \widetilde{T}_6^{11}(\eta_w,p)=-\int_{J_1}&(\eta_w)_x\big(x^+_{\frac12},y\big)\,p\big(x^+_{\frac12},y\big)dy,\quad \widetilde{T}_8^{11}(\eta_w,p)=-\int_{I_1}(\eta_w)_y\big(x,y^+_{\frac12}\big)\,p\big(x,y^+_{\frac12}\big)dx,\end{aligned}$$

and

$$\begin{aligned}B^S_{K_{11}}(w,p):=&\int_{I_1}\Big(w(x,y_{\frac12})-\mathbb{P}_{\mathrm{I}_x}\big(w(x,y_{\frac12})\big)\Big)p_y(x,y^+_{\frac12})dx\\&+\int_{J_1}\Big(w(x_{\frac12},y)-\mathbb{P}_{\mathrm{I}_y}\big(w(x_{\frac12},y)\big)\Big)p_x(x^+_{\frac12},y)dy.\end{aligned}$$

Similar to (A.2), for any $v\in H^3(\Omega_h)$ and $k\ge2$, we can obtain

$$\big|B^T_{K_{11}}(\eta_v,p)\big|\le Ch\|v\|_{3,\widetilde{K}_{11}}\|p\|_{K_{11}}, \tag{A.4}$$

where $\widetilde{K}_{11}=\{K_{21},\,K_{11},\,K_{12}\}$. Moreover, by the approximation property of the one-dimensional projection $\mathbb{P}_{\mathrm{I}}$ with $k\ge2$, trace and inverse inequalities, we get

$$\begin{aligned}|B^S_{K_{11}}(v,p)|\le&\Big|\int_{I_1}\Big(v(x,y_{\frac12})-\mathbb{P}_{\mathrm{I}_x}\big(v(x,y_{\frac12})\big)\Big)p_y(x,y^+_{\frac12})dx\Big|\\&+\Big|\int_{J_1}\Big(v(x_{\frac12},y)-\mathbb{P}_{\mathrm{I}_y}\big(v(x_{\frac12},y)\big)\Big)p_x(x^+_{\frac12},y)dy\Big|\\\le&\,Ch^3\|v\|_{3,\partial K_{11}}\|p_y\|_{\partial K_{11}}+Ch^3\|v\|_{3,\partial K_{11}}\|p_x\|_{\partial K_{11}},\\\le&\,C\big(h\|v\|_{3,K_{11}}+h^2\|v\|_{4,K_{11}}\big)\|p\|_{K_{11}}.\end{aligned} \tag{A.5}$$

Thus, for any $v\in H^4(\Omega_h)$, by virtue of (A.4) and (A.5), we arrive at the following estimate of $B_{K_{11}}(\eta_v,p)$

$$|B_{K_{11}}(\eta_v,p)|\le Ch\|v\|_{3,\widetilde{K}_{11}}\|p\|_{K_{11}}+Ch^2\|v\|_{4,K_{11}}\|p\|_{K_{11}}. \tag{A.6}$$

Besides, from Lemma 3.10 and the linearity of the operator $B_{K_{11}}(\eta_w,p)$, it follows that

$$\begin{aligned}B_{K_{11}}(\eta_w,p)=&\,B_{K_{11}}(\eta_w,p)-B_{K_{11}}(\eta_\chi,p)=B_{K_{11}}(\eta_{w-\chi},p)\\\le&\,Ch\|w-\chi\|_{3,\widetilde{K}_{11}}\|p\|_{K_{11}}+Ch^2\|w-\chi\|_{4,K_{11}}\|p\|_{K_{11}},\end{aligned}$$

holds for any $\chi \in \mathcal{P}^{k+2}$. This implies

$$\begin{aligned} B_{K_{11}}(\eta_w, p) &\le Ch\|p\|_{K_{11}} \inf_{\chi\in\mathcal{P}^{k+2}} \left(\|w-\chi\|_{3,\widetilde{K}_{11}} + h\|w-\chi\|_{4,K_{11}}\right) \\ &\le Ch^{k+1}\|p\|_{K_{11}}\|w\|_{k+3,\,\widetilde{K}_{11}}. \end{aligned}$$

Analogously, for other cases of boundary elements, we can also conclude a similar estimate, that is,

$$B_{K_{ij}}(\eta_w, p) \le Ch^{k+1}\|p\|_{K_{ij}}\|w\|_{k+3,\,\widetilde{K}_{ij}}, \quad \forall K_{ij} \in \Omega_h^0, \tag{A.7}$$

where $\widetilde{K}_{ij}$ represents the union of K_{ij} and all of its neighboring elements in Ω_h. Consequently, combining (A.3) and (A.7), and summing over all K, we get

$$\sum_{K\in\Omega_h} |B_K(\eta_w, p)| \le Ch^{k+1}\|w\|_{k+3}\|p\|.$$

This completes the proof of Lemma 3.11. □

References

[1] G. Ahlers and D.S. Cannell. Vortex-front propagation in rotating Couette–Taylor flow. *Phys. Rev. Lett.*, 50(20):1583–1586, 1983.

[2] D.G. Aronson and H.F. Weinberger. Multidimensional nonlinear diffusion arising in population genetics. *Adv. Math.*, 30(1):33–76, 1978.

[3] A. Başhan, Y. Ucar, N.M. Yağmurlu, and A. Esen. Numerical solutions for the fourth order extended Fisher–Kolmogorov equation with high accuracy by differential quadrature method. *Sigma J. Eng. Nat. Sci*, 9(3):273–284, 2018.

[4] S. Brenner. *The mathematical theory of finite element methods*. Springer, 2008.

[5] Y. Cheng and C.-W. Shu. A discontinuous Galerkin finite element method for time dependent partial differential equations with higher order derivatives. *Math. Comp.*, 77(262):699–730, 2008.

[6] P.G. Ciarlet. *The finite element method for elliptic problems*, volume 40 of *Classics in Applied Mathematics*. Society for Industrial and Applied Mathematics (SIAM), Philadelphia, PA, 2002.

[7] B. Cockburn and C.-W. Shu. The local discontinuous Galerkin method for time-dependent convection-diffusion systems. *SIAM J. Numer. Anal.*, 35(6): 2440–2463, 1998.

[8] P. Coullet, C. Elphick, and D. Repaux. Nature of spatial chaos. *Phys. Rev. Lett.*, 58(5):431–434, 1987.

[9] P. Danumjaya. Finite element methods for one dimensional fourth order semilinear partial differential equation. *Int. J. App. Comput. Math.*, 2(3):395–410, 2016.

[10] P. Danumjaya and A.K. Pani. Orthogonal cubic spline collocation method for the extended Fisher-Kolmogorov equation. *J. Comput. Appl. Math.*, 174(1):101–117, 2005.

[11] P. Danumjaya and A.K. Pani. Numerical methods for the extended Fisher-Kolmogorov (EFK) equation. *Int. J. Numer. Anal. Model.*, 3(2):186–210, 2006.

[12] P. Danumjaya and A.K. Pani. Mixed finite element methods for a fourth order reaction diffusion equation. *Numer. Methods Partial Differ. Equ.*, 28(4):1227–1251, 2012.

[13] G.T. Dee and W. van Saarloos. Bistable systems with propagating fronts leading to pattern formation. *Phys. Rev. Lett.*, 60(25):2641–2644, 1988.

[14] V. Dolejší and M. Feistauer. *Discontinuous Galerkin method. Analysis and applications to compressible flow*, volume 48 of *Springer Ser. Comput. Math.* Springer, Cham, 2015.

[15] B. Dong and C.-W. Shu. Analysis of a local discontinuous Galerkin method for linear time-dependent fourth-order problems. *SIAM J. Numer. Anal.*, 47(5):3240–3268, 2009.

[16] L.J.T. Doss and A.P. Nandini. An H^1-Galerkin mixed finite element method for the extended Fisher-Kolmogorov equation. *Int. J. Numer. Anal. Model. Ser. B*, 3(4):460–485, 2012.

[17] R.A. Fisher. The wave of advance of advantageous genes. *Ann. Eugen.*, 7(4):355–369, 1937.

[18] F. Fu, C.W. Shu, Q. Tao, and B. Wu. Analysis of the boundary conditions for the ultraweak-local discontinuous Galerkin method of time-dependent linear fourth-order problems. *Math. Comp.*, 94(351):123–158, 2025.

[19] T. Gudi and H.S. Gupta. A fully discrete C^0 interior penalty Galerkin approximation of the extended Fisher–Kolmogorov equation. *J. Comput. Appl. Math.*, 247:1–16, 2013.

[20] R.M. Hornreich, M. Luban, and S. Shtrikman. Critical behavior at the onset of $\vec{k}$-space instability on the λ line. *Phys. Rev. Lett.*, 35(25):1678–1681, 1975.

[21] T. Kadri and K. Omrani. A second-order accurate difference scheme for an extended Fisher–Kolmogorov equation. *Comput. Math. Appl.*, 61(2):451–459, 2011.

[22] N. Khiari and K. Omrani. Finite difference discretization of the extended Fisher–Kolmogorov equation in two dimensions. *Comput. Math. Appl.*, 62(11):4151–4160, 2011.

[23] A.N. Kolmogorov. A study of the equation of diffusion with increase in the quantity of matter, and its application to a biological problem. *Mosc. Univ. Math. Bull.*, 1:1–25, 1937.

[24] S. Li, D. Xu, J. Zhang, and C. Sun. A new three-level fourth-order compact finite difference scheme for the extended Fisher–Kolmogorov equation. *Appl. Numer. Math.*, 178:41–51, 2022.

[25] L. Pei and D. Shi. A new error analysis of nonconforming Bergan's energy-orthogonal element for the extended Fisher-Kolmogorov equation. *J. Math. Anal. Appl.*, 464(2):1383–1407, 2018.

[26] L.A. Peletier and W.C. Troy. Chaotic spatial patterns described by the extended Fisher–Kolmogorov equation. *J. Differ. Equ.*, 129(2):458–508, 1996.

[27] L.A. Peletier and W.C. Troy. Spatial patterns described by the extended Fisher–Kolmogorov equation: Periodic solutions. *SIAM J. Math. Anal.*, 28(6):1317–1353, 1997.

[28] V. Rottschäfer and A. Doelman. On the transition from the Ginzburg–Landau equation to the extended Fisher–Kolmogorov equation. *Physica D*, 118(3-4):261–292, 1998.

[29] C.-W. Shu. *Discontinuous Galerkin method for time-dependent problems: survey and recent developments*, volume 157 of *IMA Vol. Math. Appl.* Springer, Cham, 2014.

[30] Q. Tao, Y. Xu, and C.-W. Shu. An ultraweak-local discontinuous Galerkin method for PDEs with high order spatial derivatives. *Math. Comp.*, 89(326):2753–2783, 2020.

[31] W. van Saarloos. Front propagation into unstable states. II. linear versus nonlinear marginal stability and rate of convergence. *Phys. Rev. A*, 39(12):6367–6389, 1989.

[32] Y.L. Zhao and X.M. Gu. An adaptive low-rank splitting approach for the extended Fisher–Kolmogorov equation. *J. Comput. Phys.*, 506:112925, 2024.

[33] G. Zhu. Experiments on director waves in nematic liquid crystals. *Phys. Rev. Lett.*, 49(18):1332–1335, 1982.

[34] W. Zimmermann. Propagating fronts near a Lifshitz point. *Phys. Rev. Lett.*, 66(11):1546, 1991.